Supporting Information

for

Probing the Limits of Oxidative Addition of C(sp^3)-X Bonds Toward Selected *N,C,N*-Chelated Bismuth(I) Compounds.

Martin Hejda,[a] Robert Jirásko,[b] Aleš Růžička,[a] Roman Jambor[a] and Libor Dostál[a]

[a] *Department of General and Inorganic Chemistry, University of Pardubice, Studentská 573, CZ 532 10 Pardubice, Czech Republic.*

[b] *Department of Analytical Chemistry, University of Pardubice, Studentská 573, CZ 532 10 Pardubice, Czech Republic.*

Contents

NMR spectra of isolated compounds.

Figure S1. ^{1}H NMR spectrum of **1a** (500 MHz, CD_3CN, 298 K).

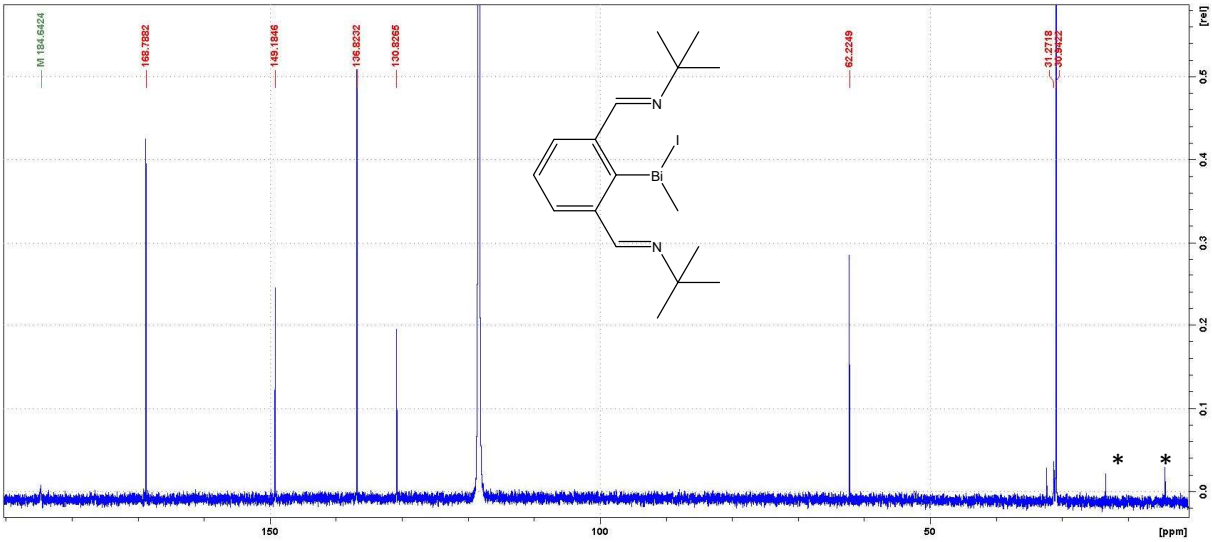

Figure S2. ^{13}C{^{1}H} NMR spectrum of **1a** (125.76 MHz, CD_3CN, 298 K). *denotes traces of hexane.

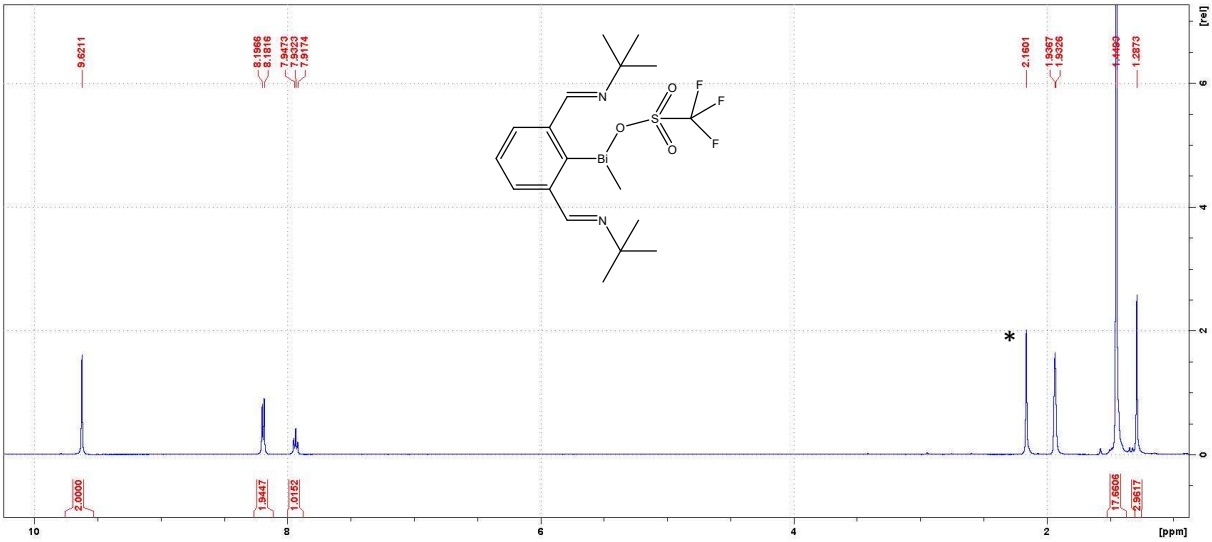

Figure S3. ^{1}H NMR spectrum of **1b** (500 MHz, CD_3CN, 298 K). *denotes traces of residual moisture in CD_3CN.

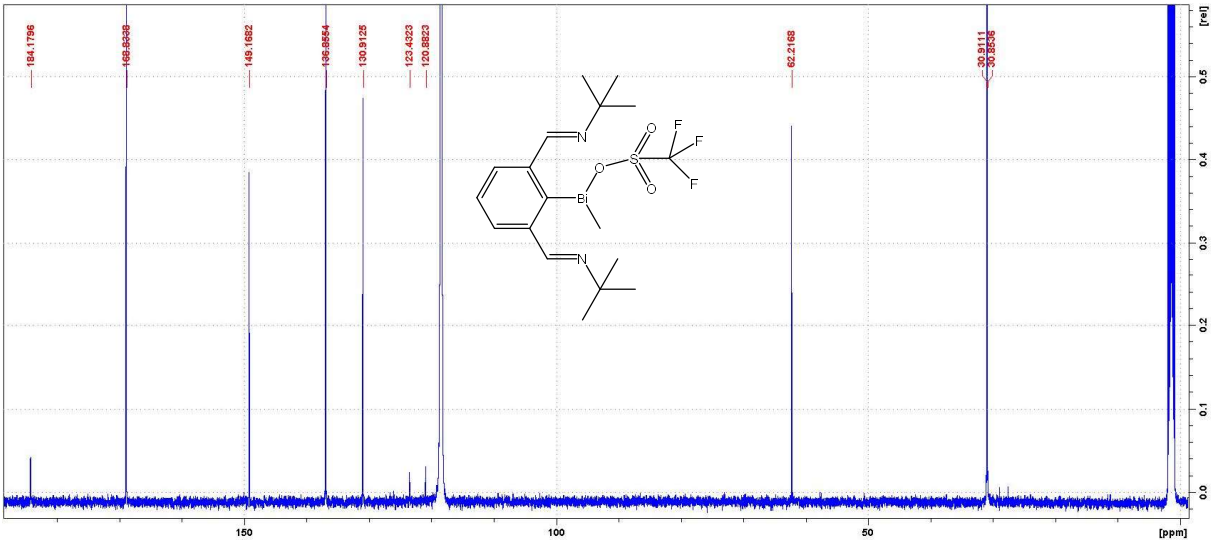

Figure S4. ^{13}C{^{1}H} NMR spectrum of **1b** (125.76 MHz, CD_3CN, 298 K).

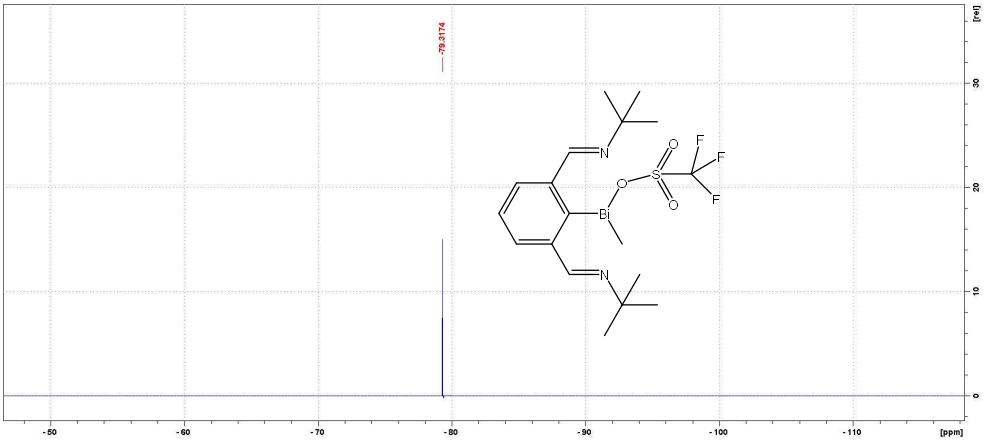

Figure S5. ^{19}F{^{1}H} NMR spectrum of **1b** (376.5 MHz, CD_3CN, 298 K).

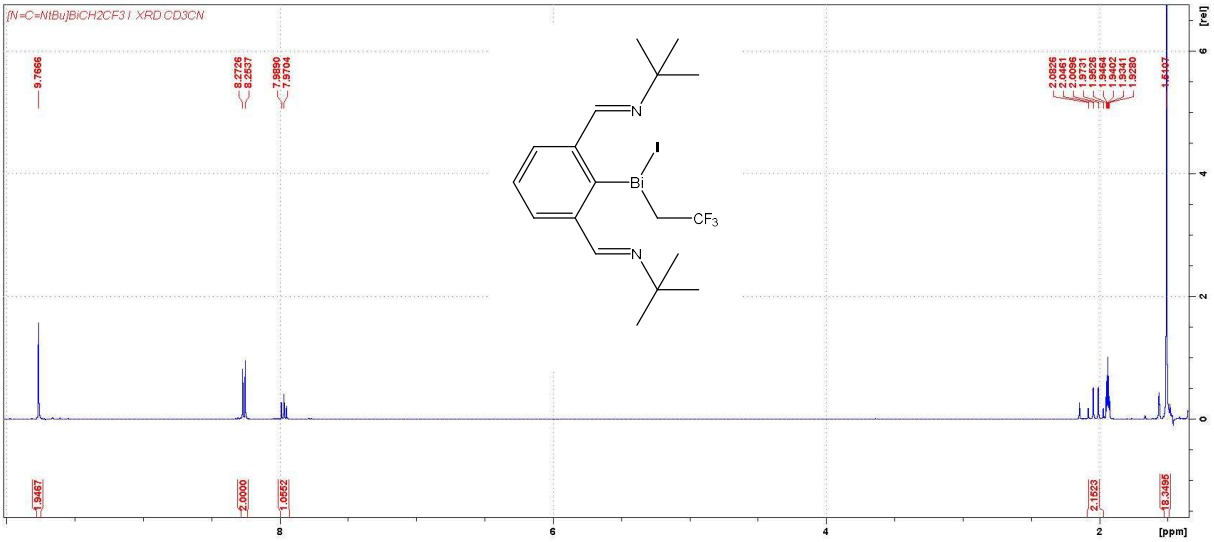

Figure S6. ^{1}H NMR spectrum of **1c** (400 MHz, CD_3CN, 298 K).

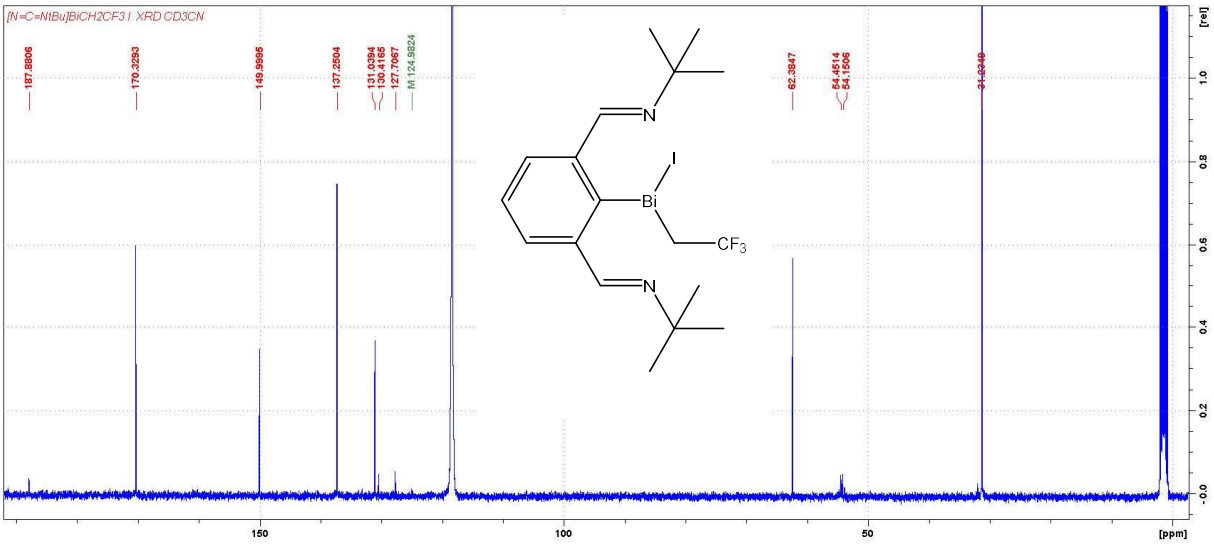

Figure S7. ^{13}C{^{1}H} NMR spectrum of **1c** (101.61 MHz, CD_3CN, 298 K).

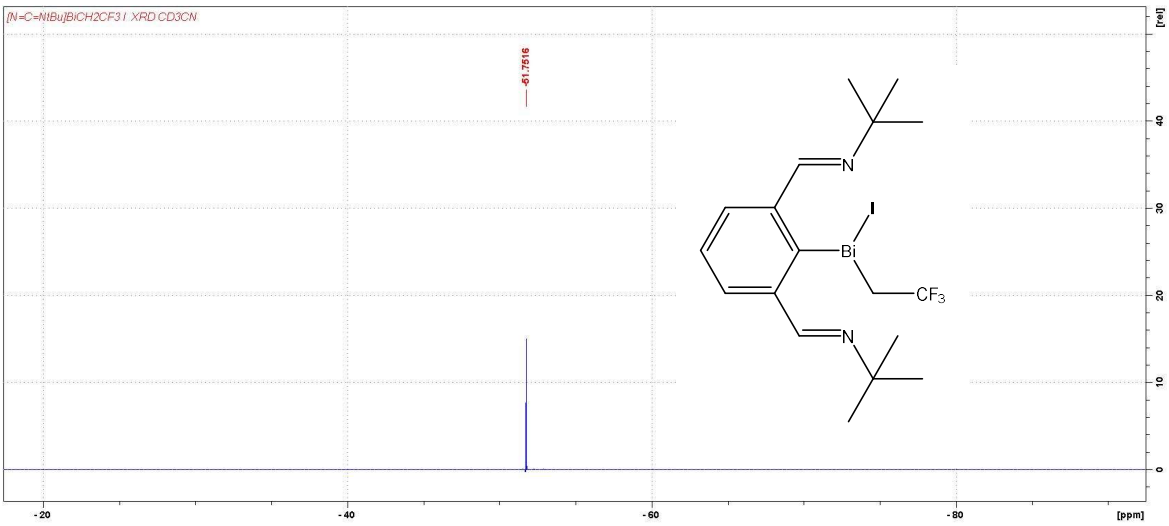

Figure S8. ^{19}F{^{1}H} NMR spectrum of **1c** (376.5 MHz, CD_3CN, 298 K).

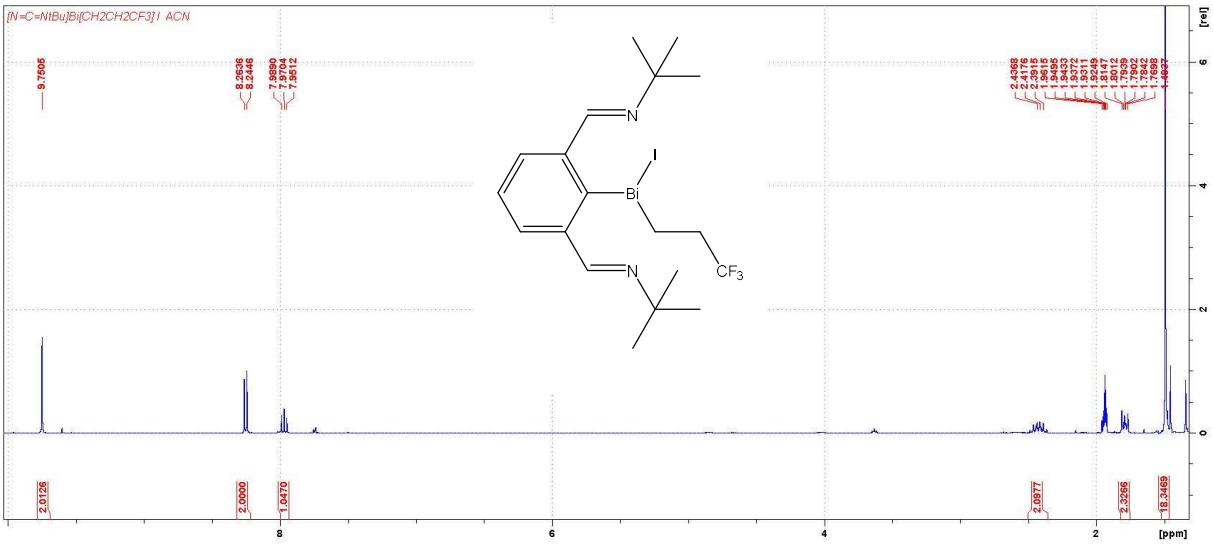

Figure S9. ^{1}H NMR spectrum of **1d** (400 MHz, CD_3CN, 298 K).

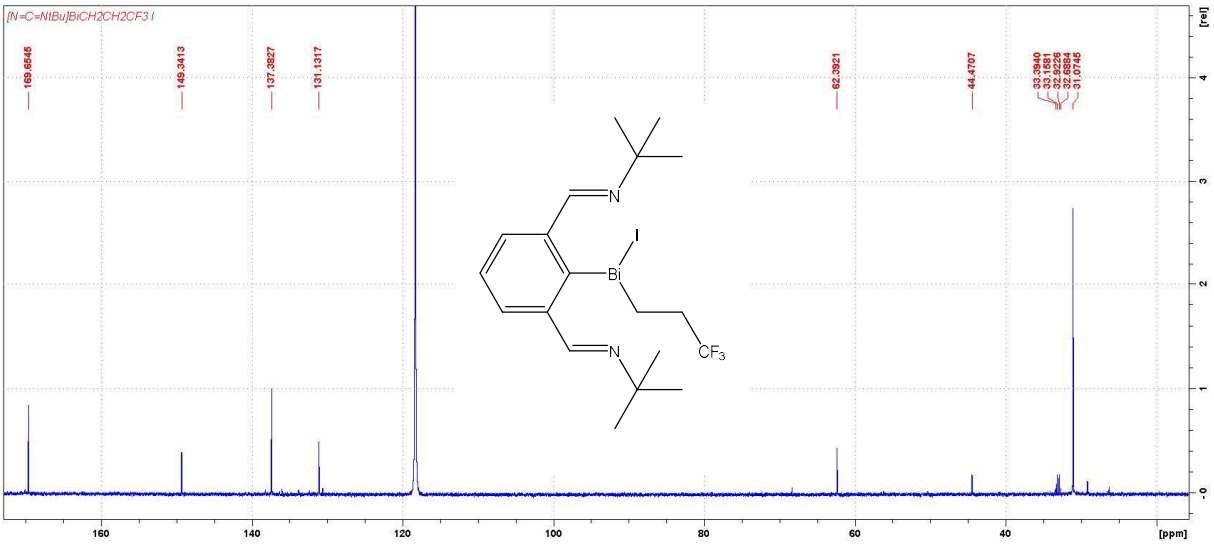

Figure S10. ^{13}C{^{1}H} NMR spectrum of **1d** (125.76 MHz, CD_3CN, 298 K).

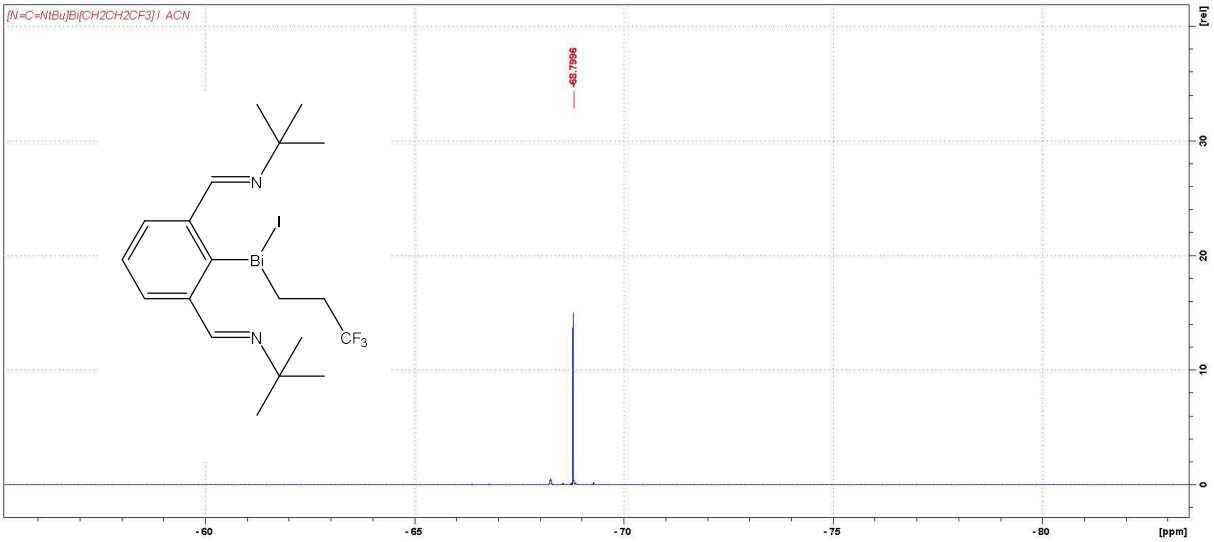

Figure S11. $^{19}F\{^{1}H\}$ NMR spectrum of **1d** (376.5 MHz, CD_3CN, 298 K).

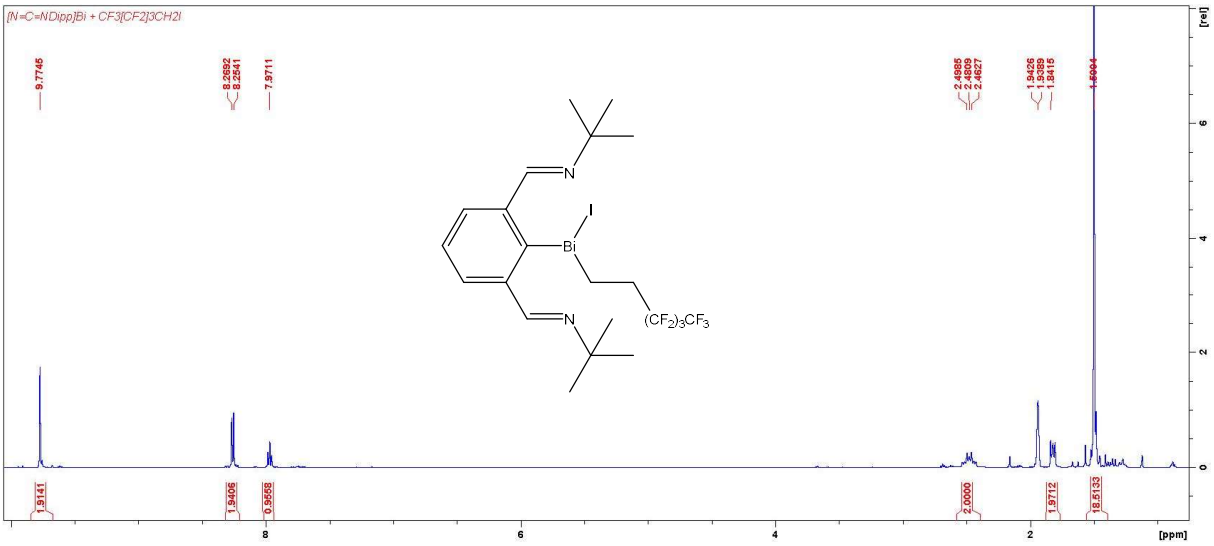

Figure S12. ^{1}H NMR spectrum of **1e** (500 MHz, CD_3CN, 298 K).

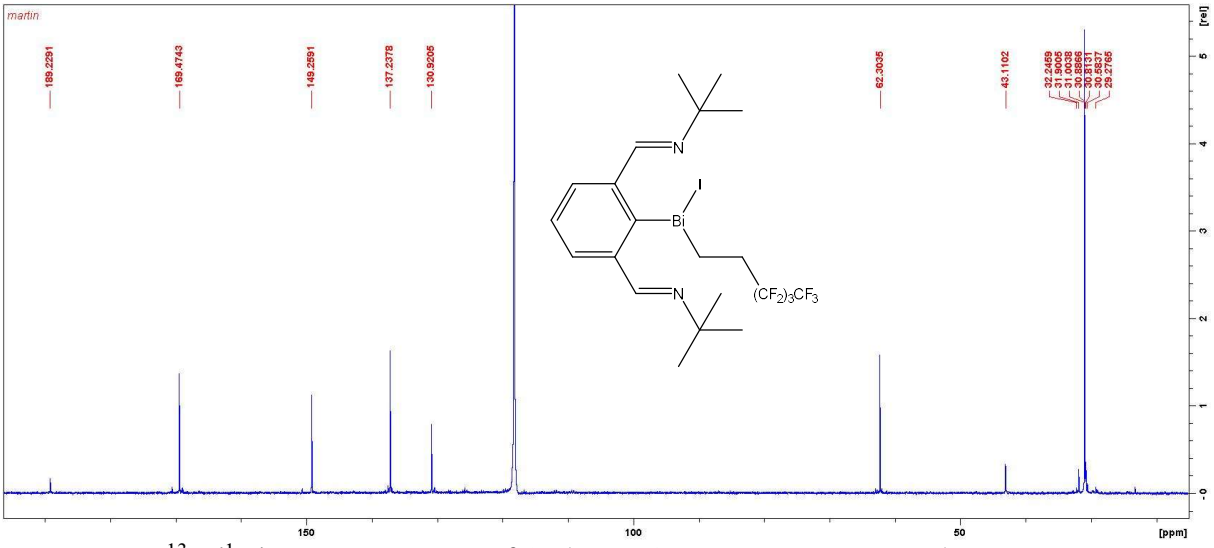

Figure S13. $^{13}C\{^{1}H\}$ NMR spectrum of **1e** (125.76 MHz, CD_3CN, 298 K).

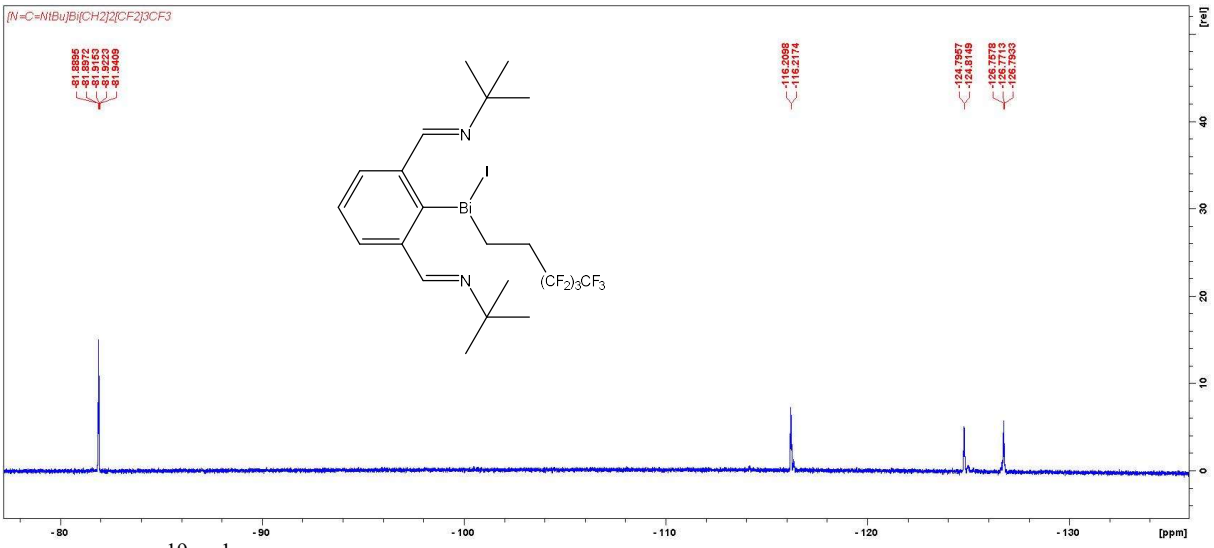

Figure S14. $^{19}F\{^{1}H\}$ NMR spectrum of **1e** (376.5 MHz, CD_3CN, 298 K).

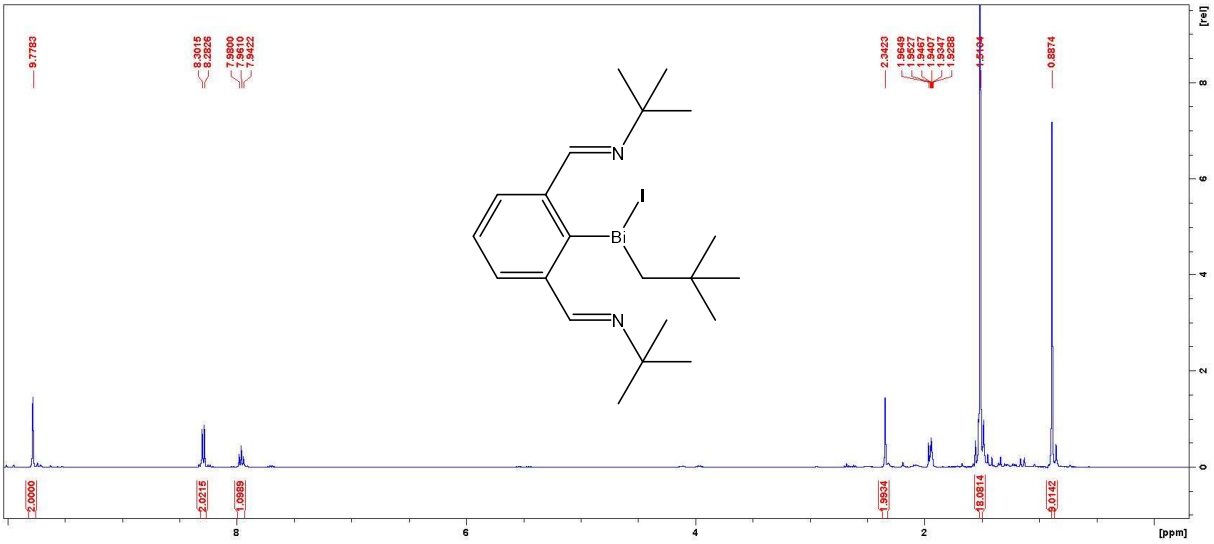

Figure S15. ^{1}H NMR spectrum of **1f** (500 MHz, CD_3CN, 298 K).

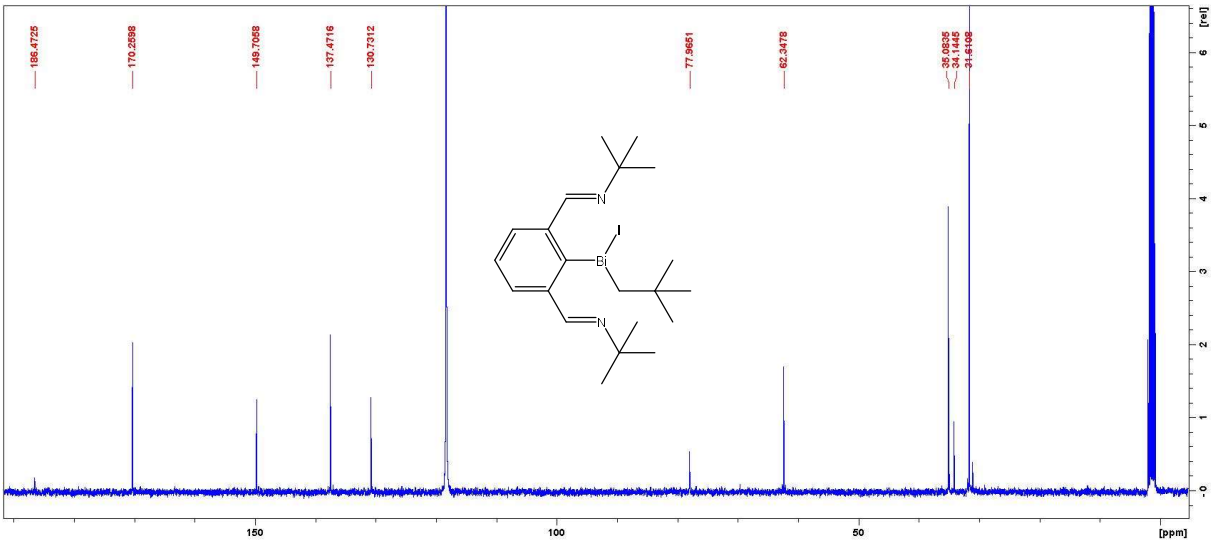

Figure S16. $^{13}C\{^{1}H\}$ NMR spectrum of **1f** (125.76 MHz, CD_3CN, 298 K).

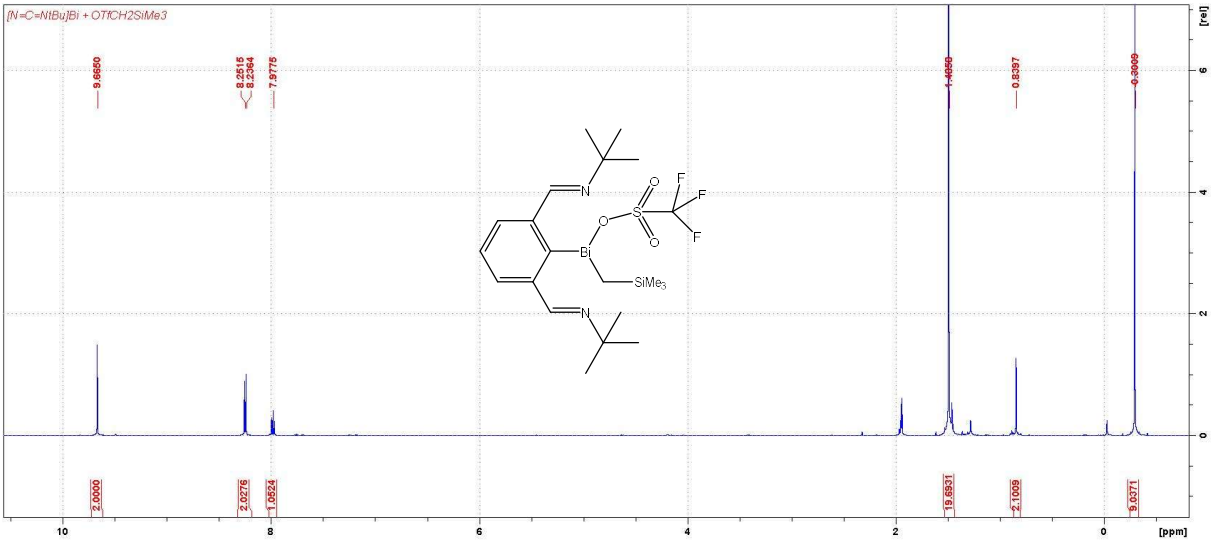

Figure S17. ^{1}H NMR spectrum of **1g** (500 MHz, CD_3CN, 298 K).

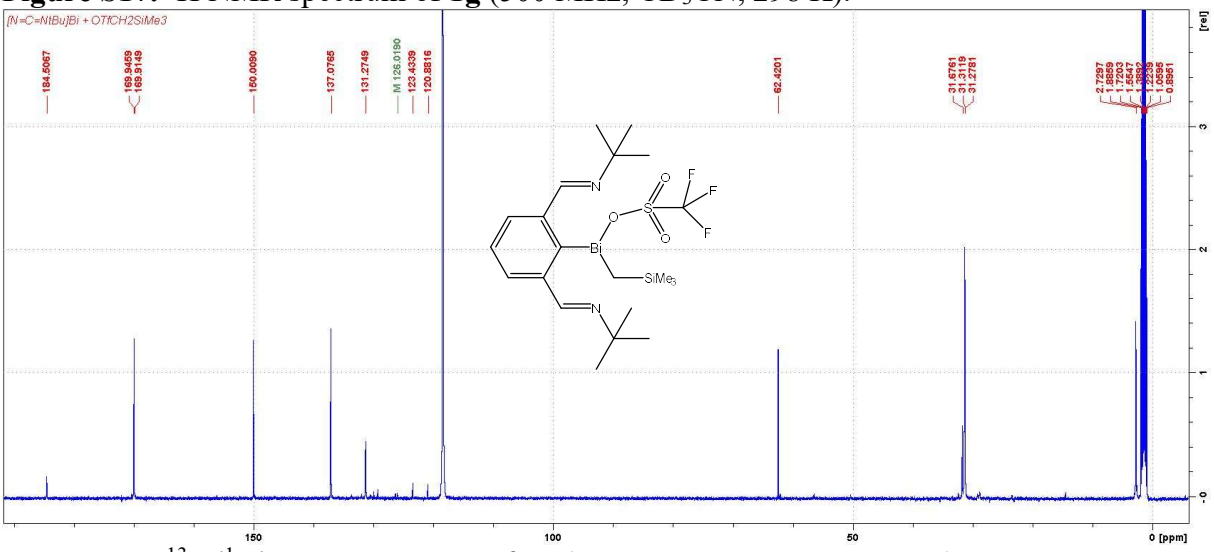

Figure S18. ^{13}C{^{1}H} NMR spectrum of **1g** (125.76 MHz, CD_3CN, 298 K).

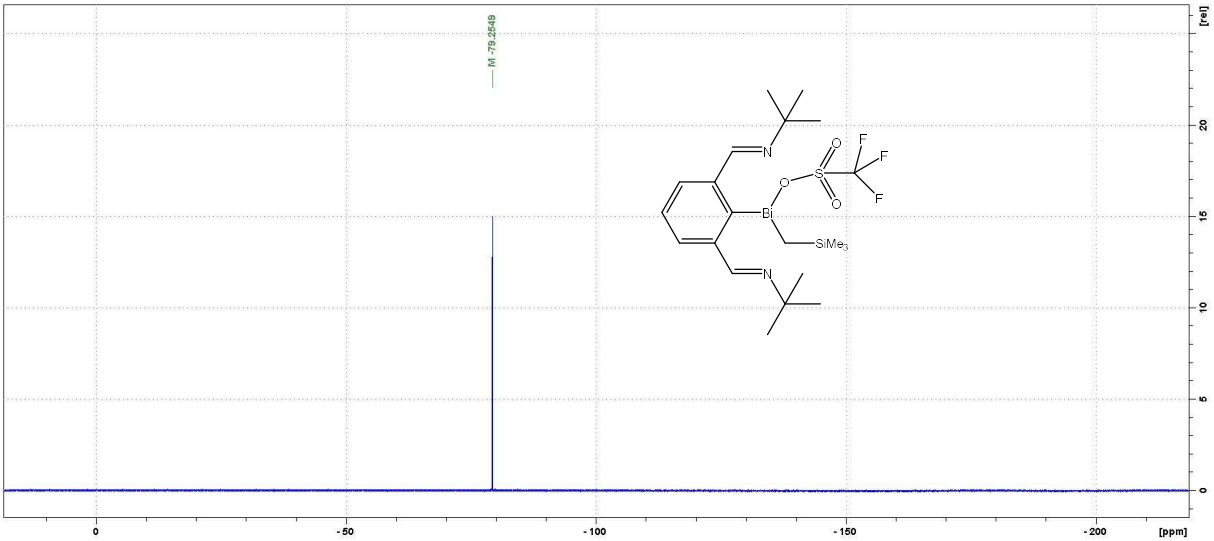

Figure S19. $^{19}F\{^{1}H\}$ NMR spectrum of **1g** (376.5 MHz, CD_3CN, 298 K).

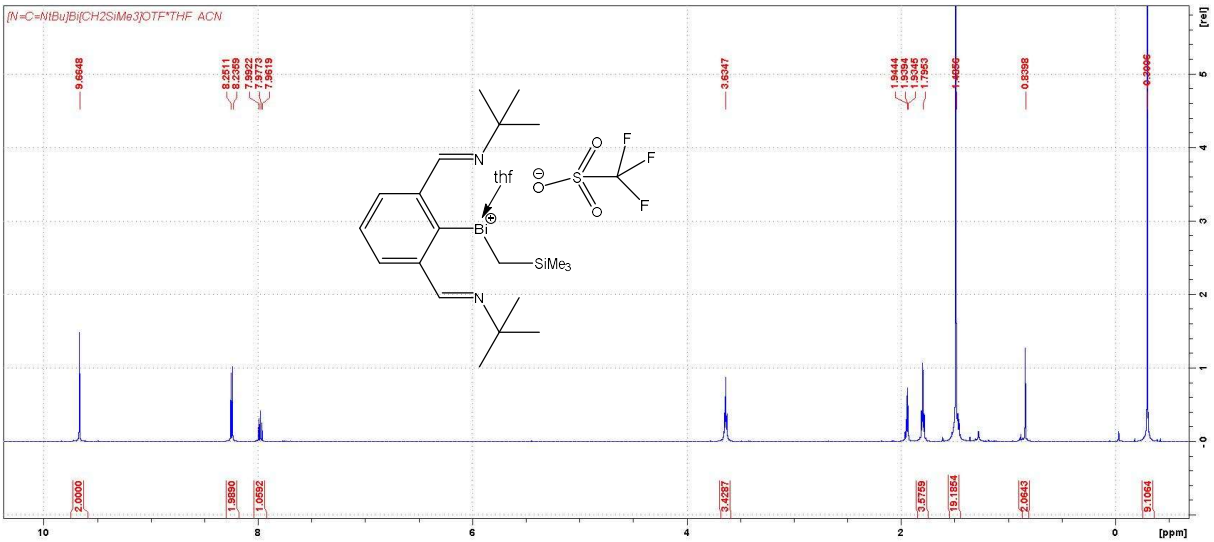

Figure S20. ^{1}H NMR spectrum of **1g.thf** (single crystals) (500 MHz, CD_3CN, 298 K).

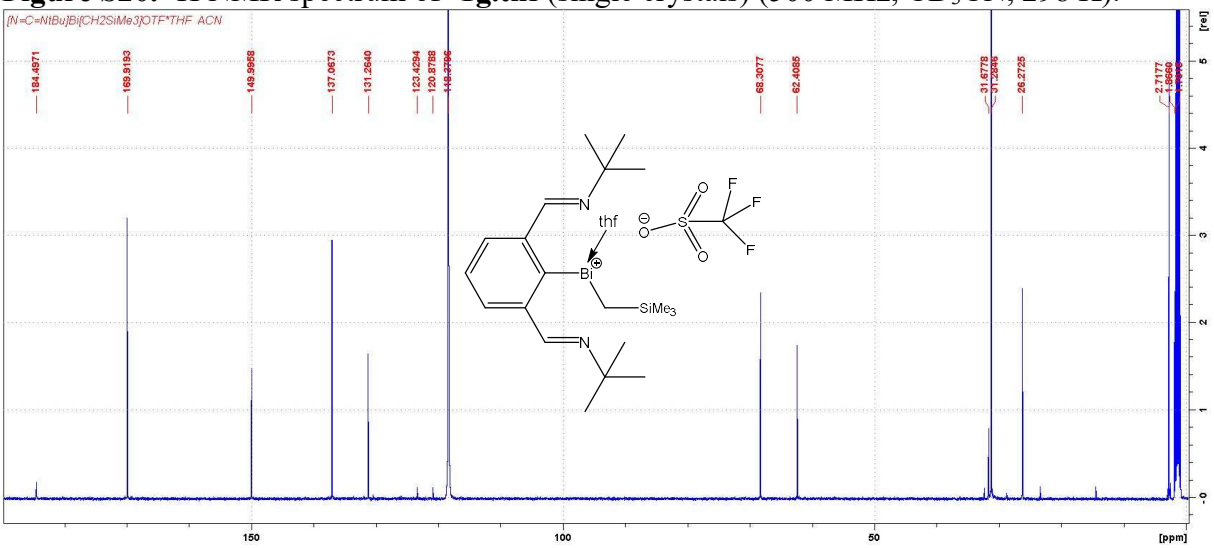

Figure S21. $^{13}C\{^{1}H\}$ NMR spectrum of **1g.thf** (single crystals) (125.76 MHz, CD_3CN, 298 K).

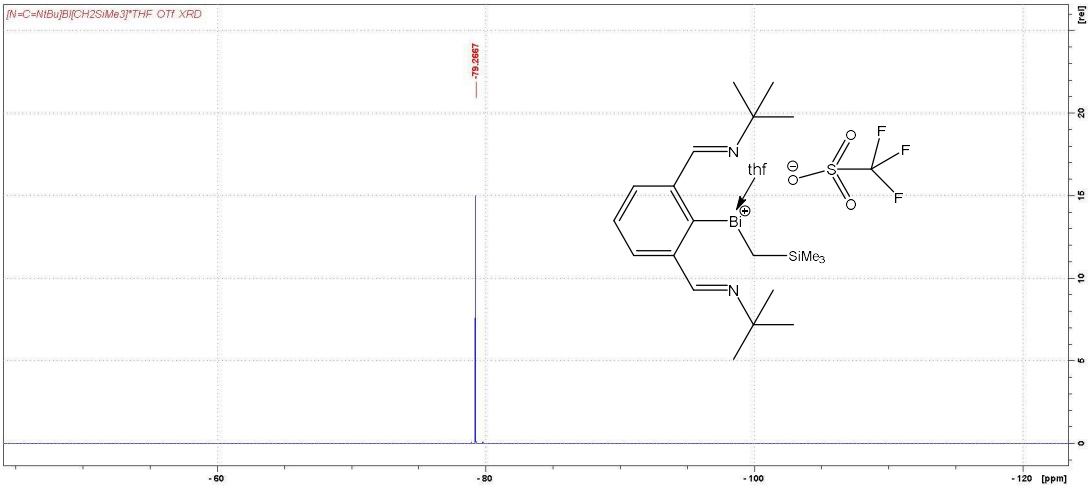

Figure S22. $^{19}F\{^{1}H\}$ NMR spectrum of **1g.thf** (single crystals) (376.5 MHz, CD_3CN, 298 K).

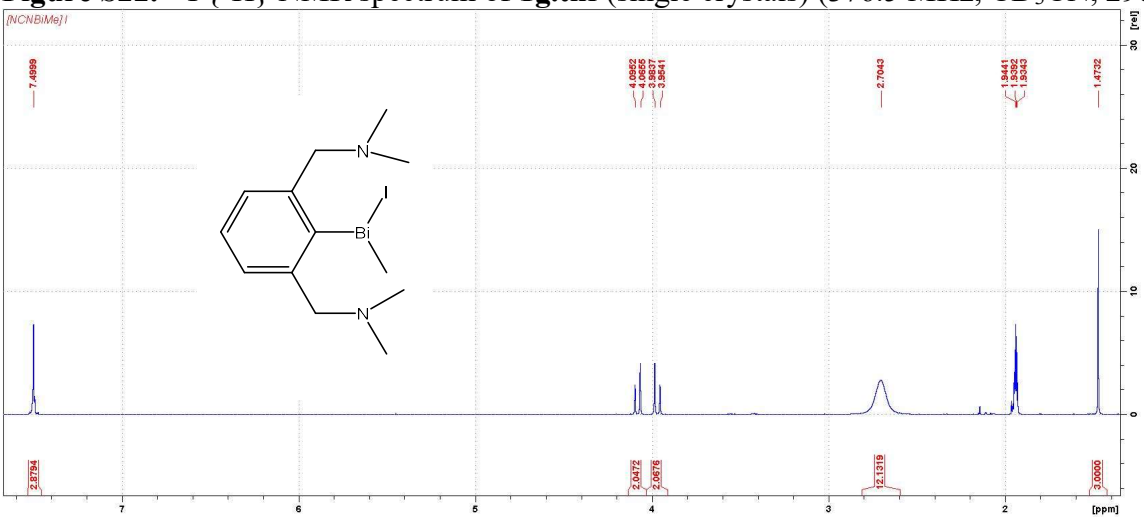

Figure S23. ^{1}H NMR spectrum of **2a** (500 MHz, CD_3CN, 298 K)

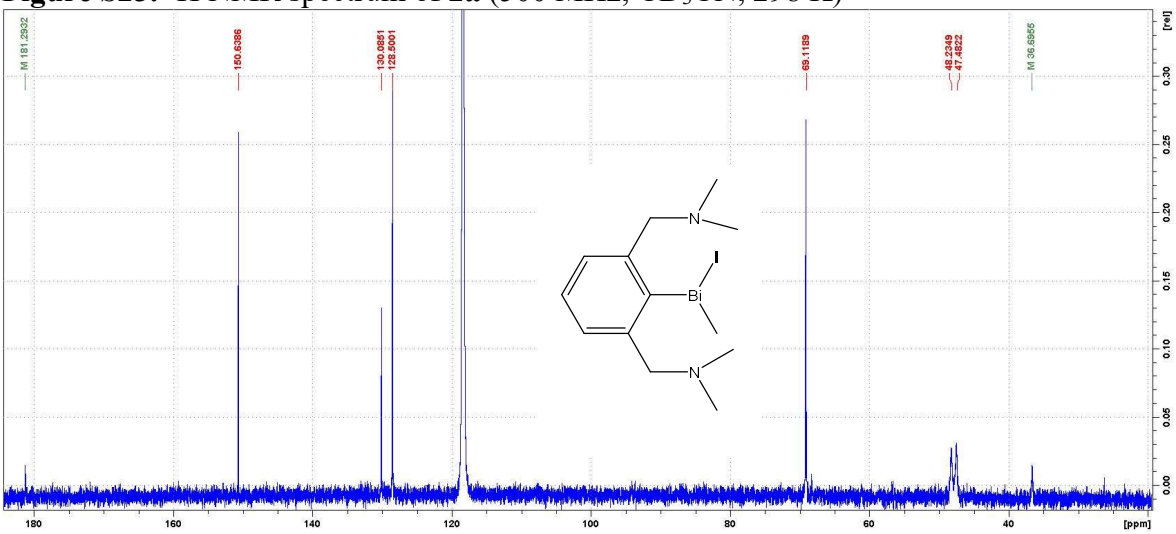

Figure S24. $^{13}C\{^{1}H\}$ NMR spectrum of **2a** (125.76 MHz, CD_3CN, 298 K).

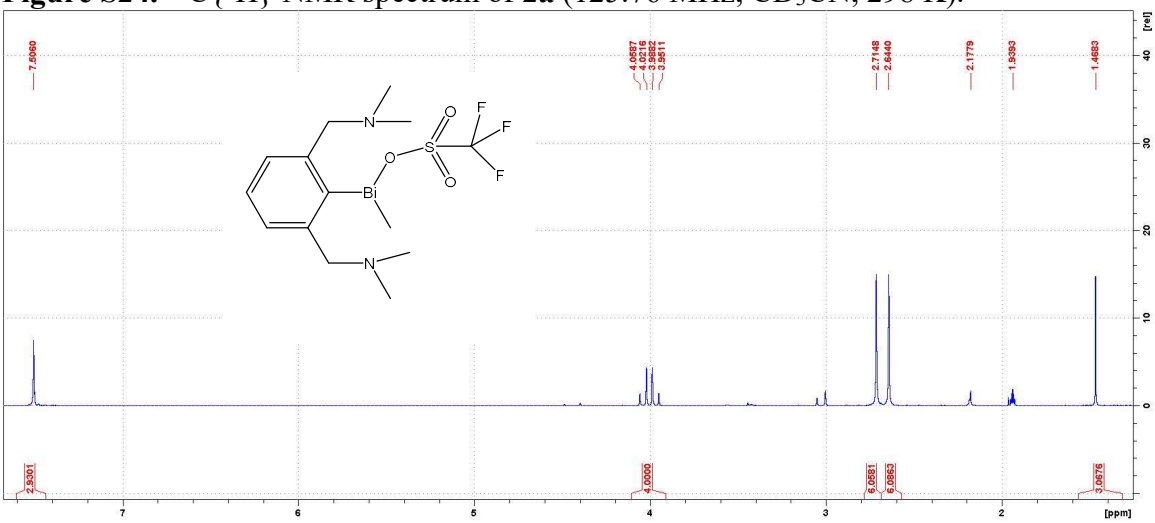

Figure S25. ^{1}H NMR spectrum of **2b** (400 MHz, CD_3CN, 298 K),

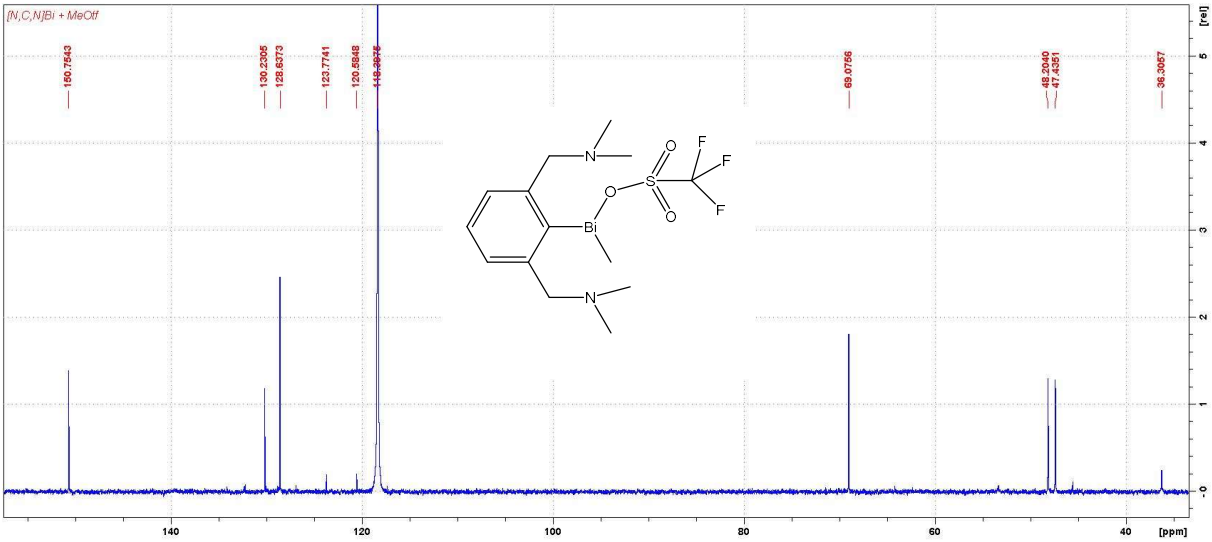

Figure S26. $^{13}C\{^{1}H\}$ NMR spectrum of **2b** (100.61 MHz, CD_3CN, 298 K).

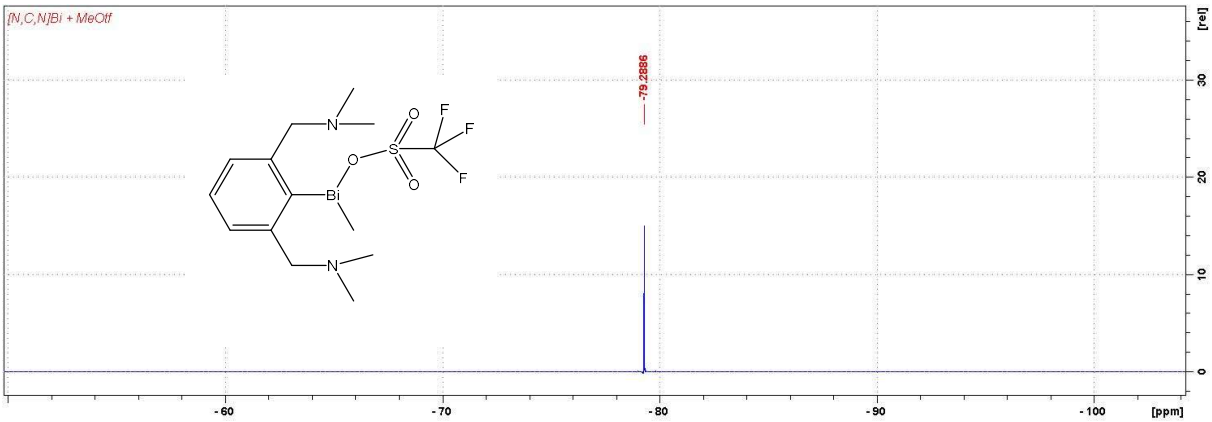

Figure S27. $^{19}F\{^{1}H\}$ NMR spectrum of **2b** (376.5 MHz, CD_3CN, 298 K).

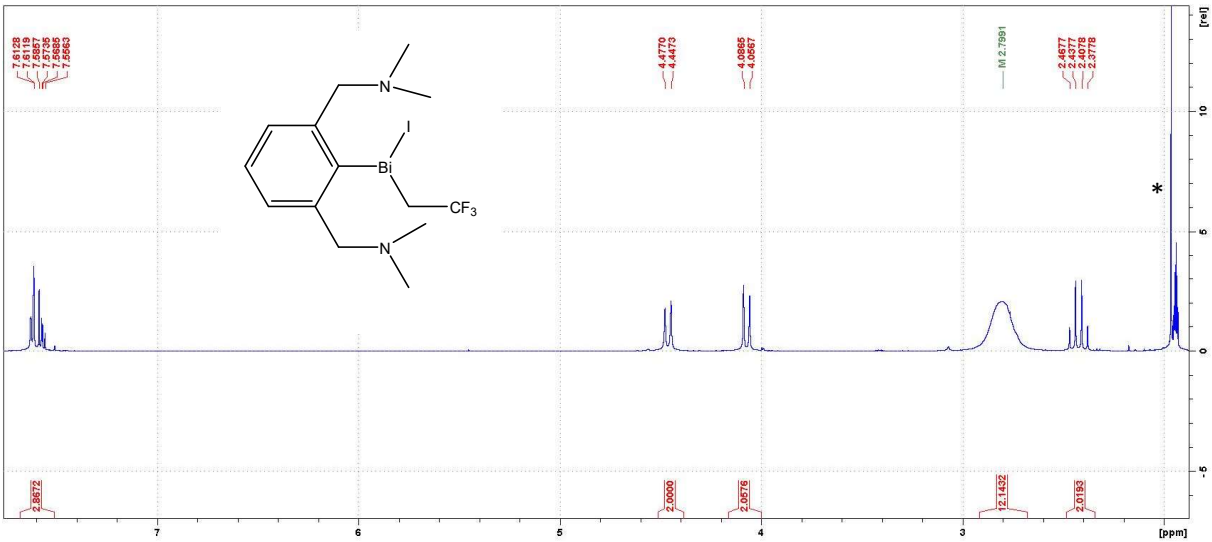

Figure S28. ^{1}H NMR spectrum of **2c** (500 MHz, CD_3CN, 298 K). *denotes traces CH_3CN used for crystallization.

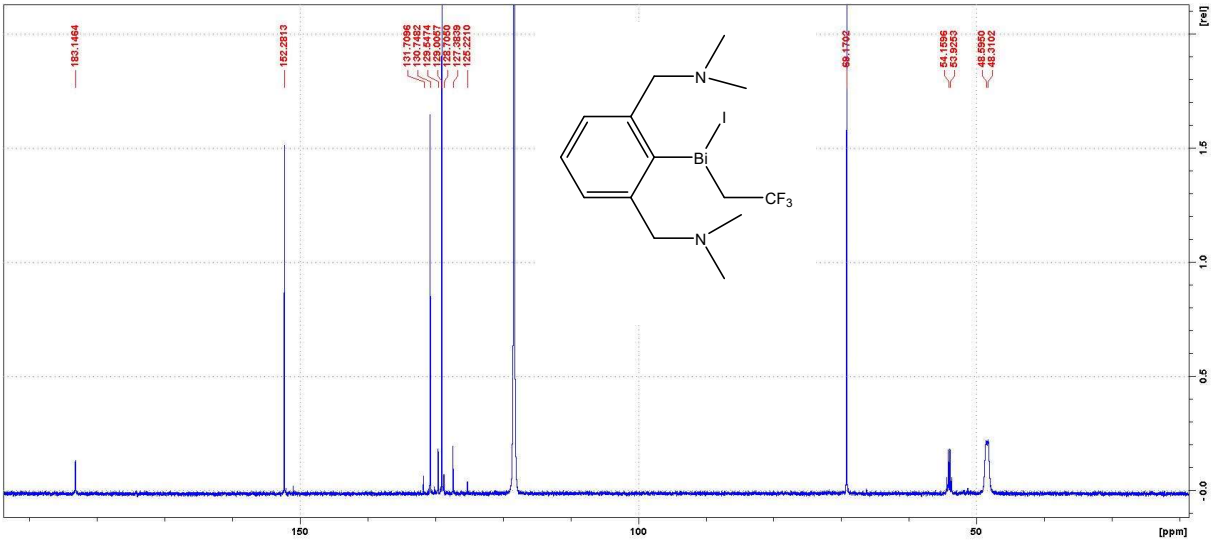

Figure S29. $^{13}C\{^{1}H\}$ NMR spectrum of **2c** (125.76 MHz, CD_3CN, 298 K).

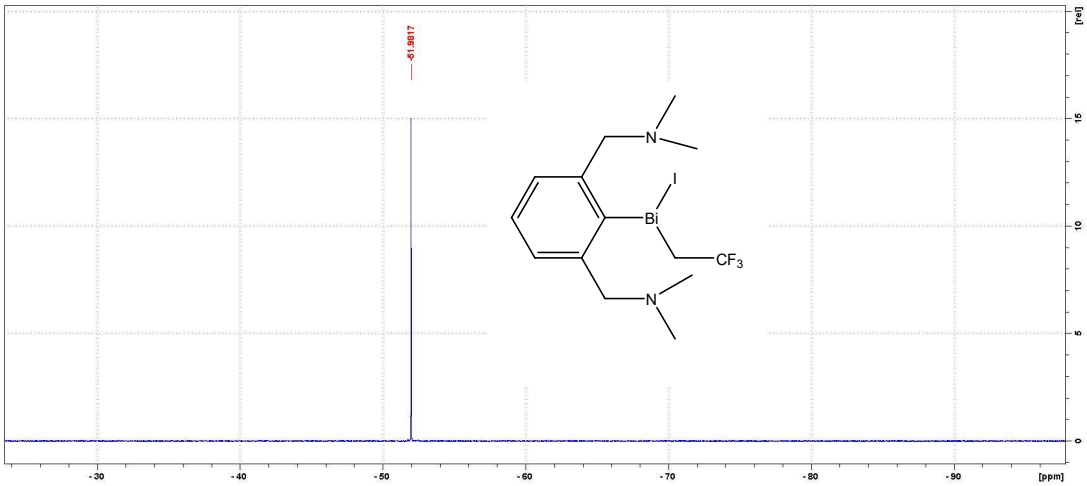

Figure S30. $^{19}F\{^{1}H\}$ NMR spectrum of **2c** (376.5 MHz, CD_3CN, 298 K).

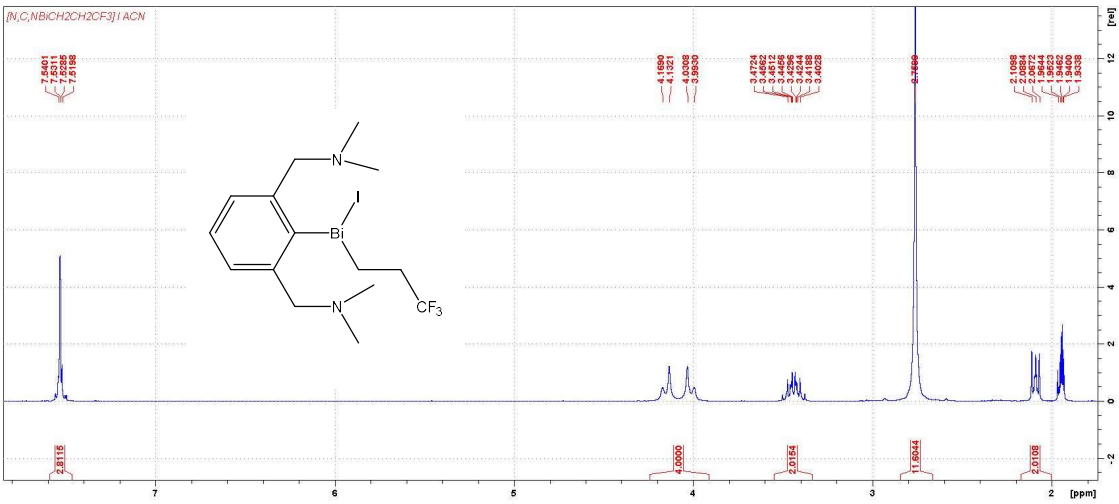

Figure S31. ^{1}H NMR spectrum of **2d** (400 MHz, CD_3CN, 298 K).

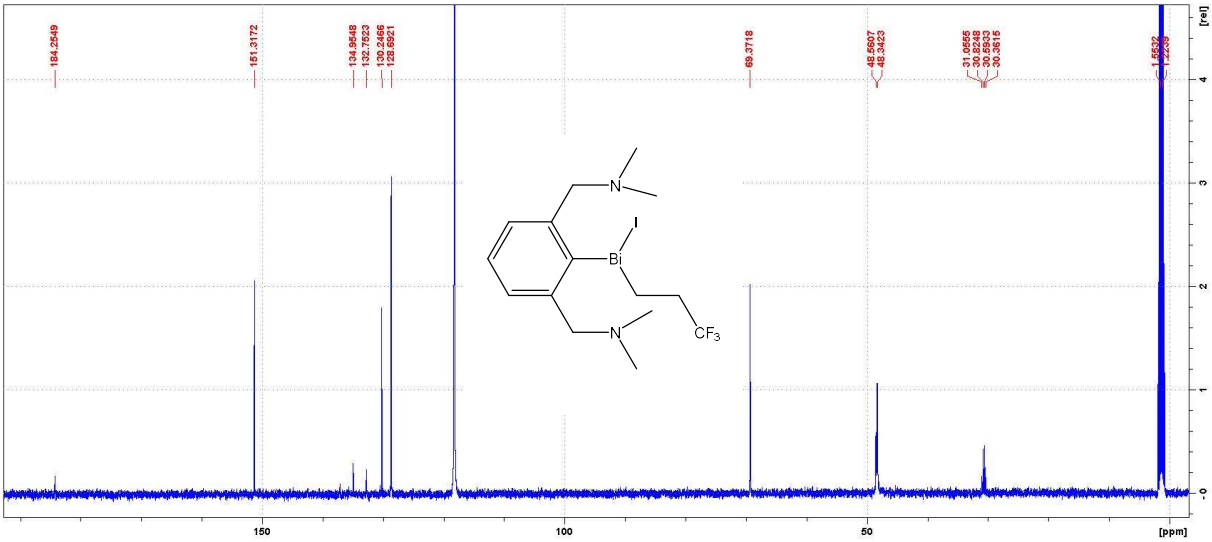

Figure S32. $^{13}C\{^{1}H\}$ NMR spectrum of **2d** (125.76 MHz, CD_3CN, 298 K).

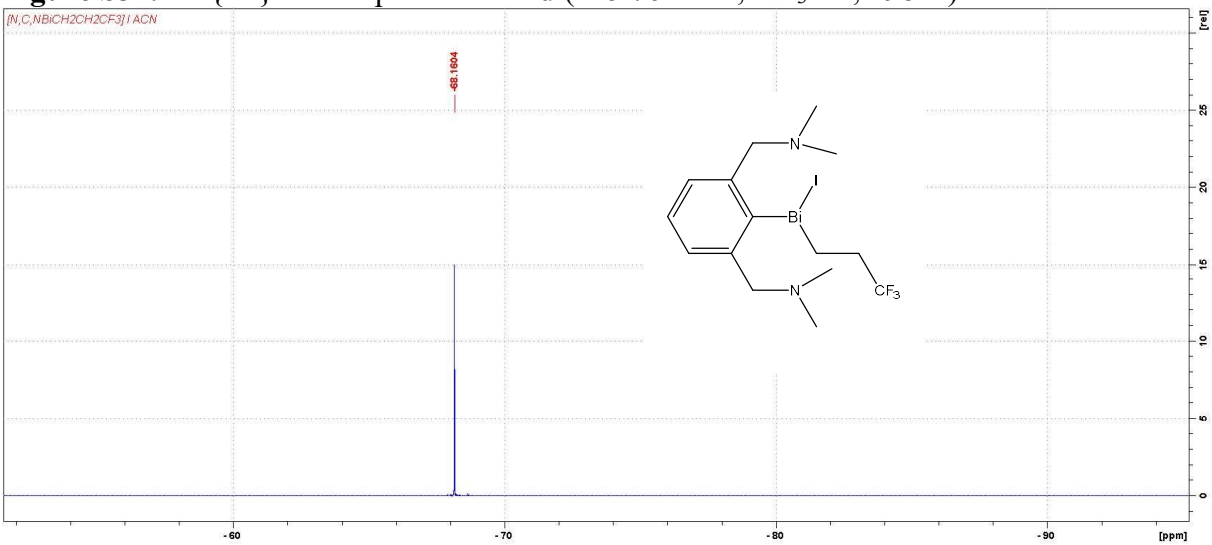

Figure S33. $^{19}F\{^{1}H\}$ NMR spectrum of **2c** (376.5 MHz, CD_3CN, 298 K).

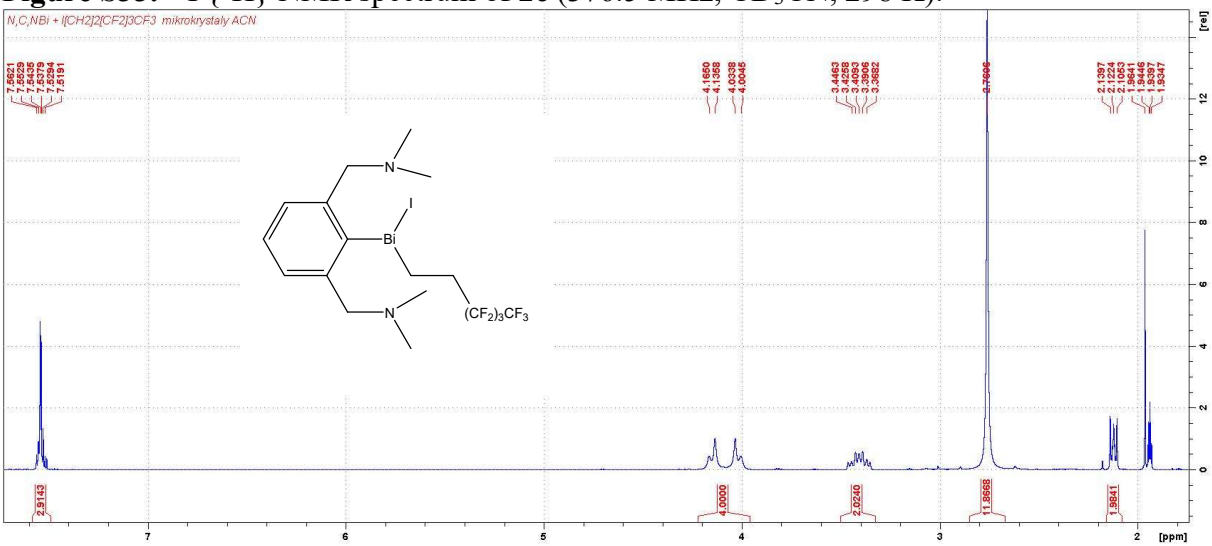

Figure S34. ^{1}H NMR spectrum of **2e** (500 MHz, CD_3CN, 298 K).

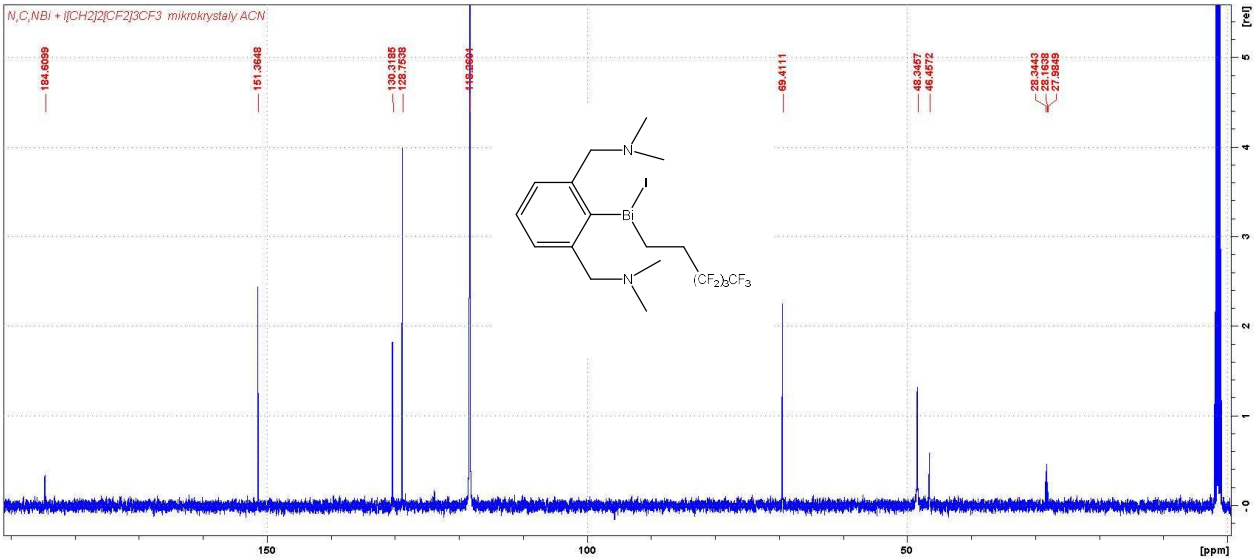

Figure S35. $^{13}C\{^{1}H\}$ NMR spectrum of **2e** (125.76 MHz, CD_3CN, 298 K).

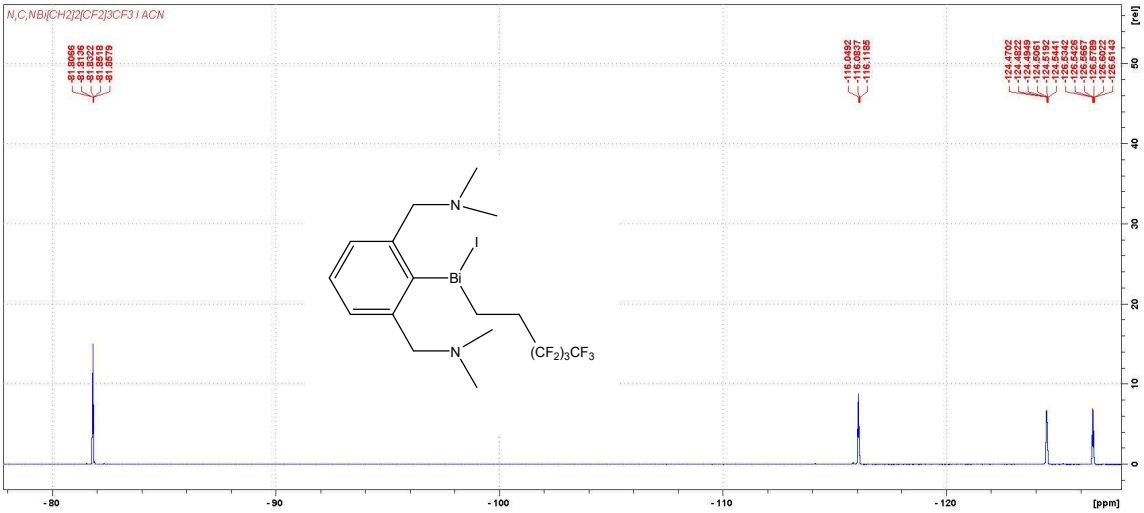

Figure S36. $^{19}F\{^{1}H\}$ NMR spectrum of **2e** (376.5 MHz, CD_3CN, 298 K).

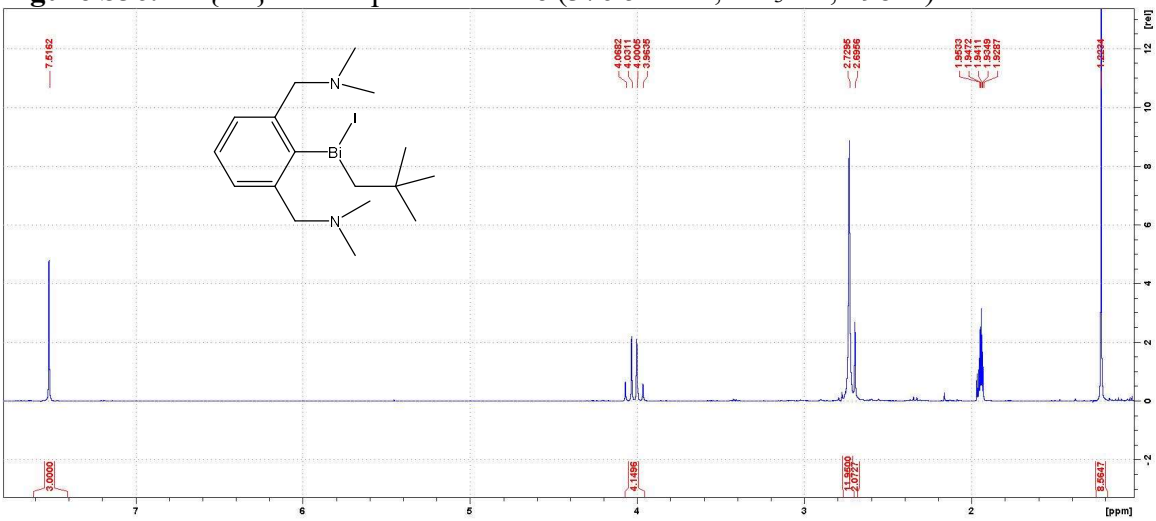

Figure S37. ^{1}H NMR spectrum of **2f** (500 MHz, CD_3CN, 298 K).

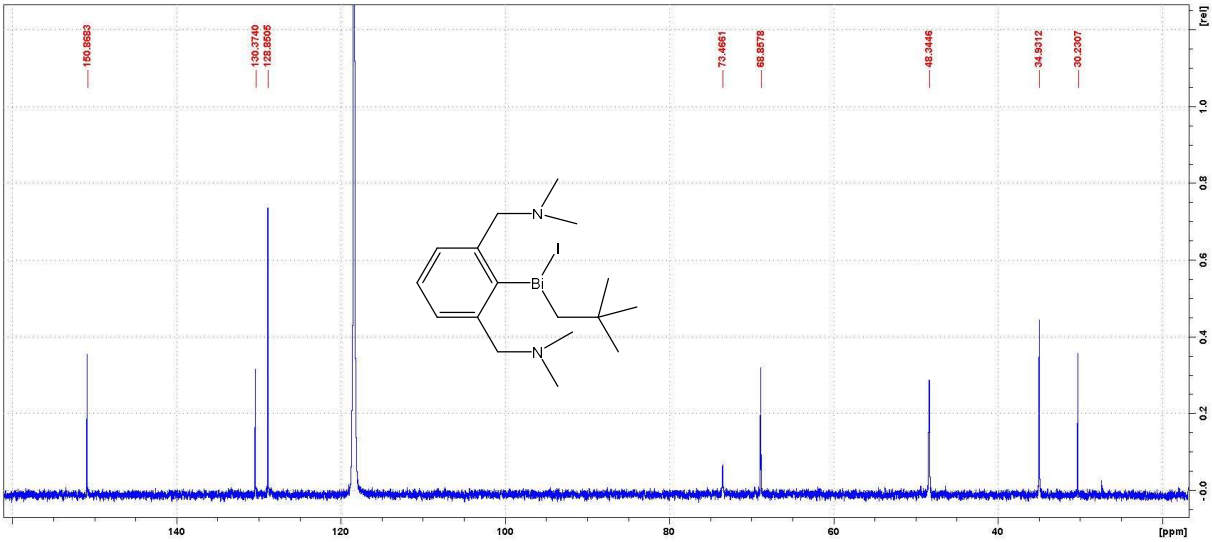

Figure S38. $^{13}C\{^{1}H\}$ NMR spectrum of **2f** (125.76 MHz, CD_3CN, 298 K).

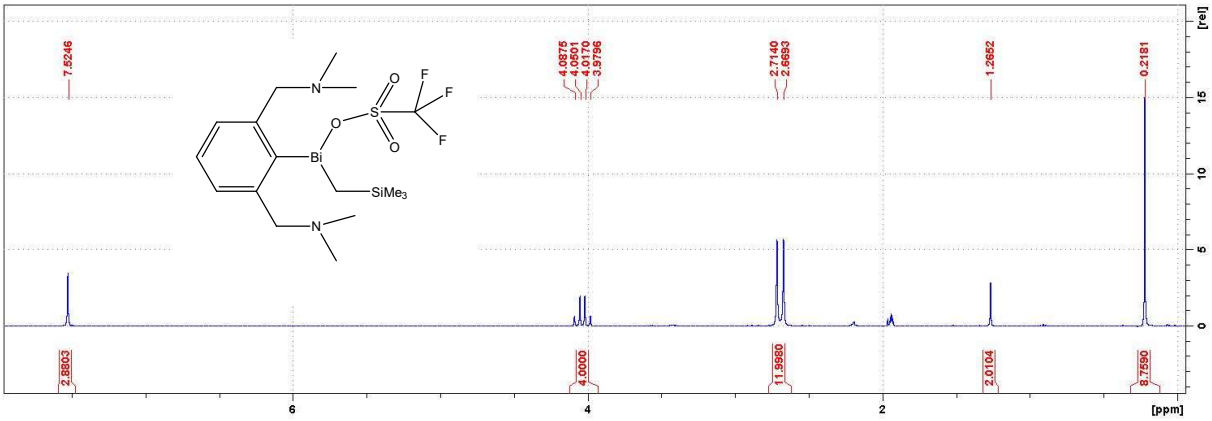

Figure S39. ^{1}H NMR spectrum of **2g** (400 MHz, CD_3CN, 298 K).

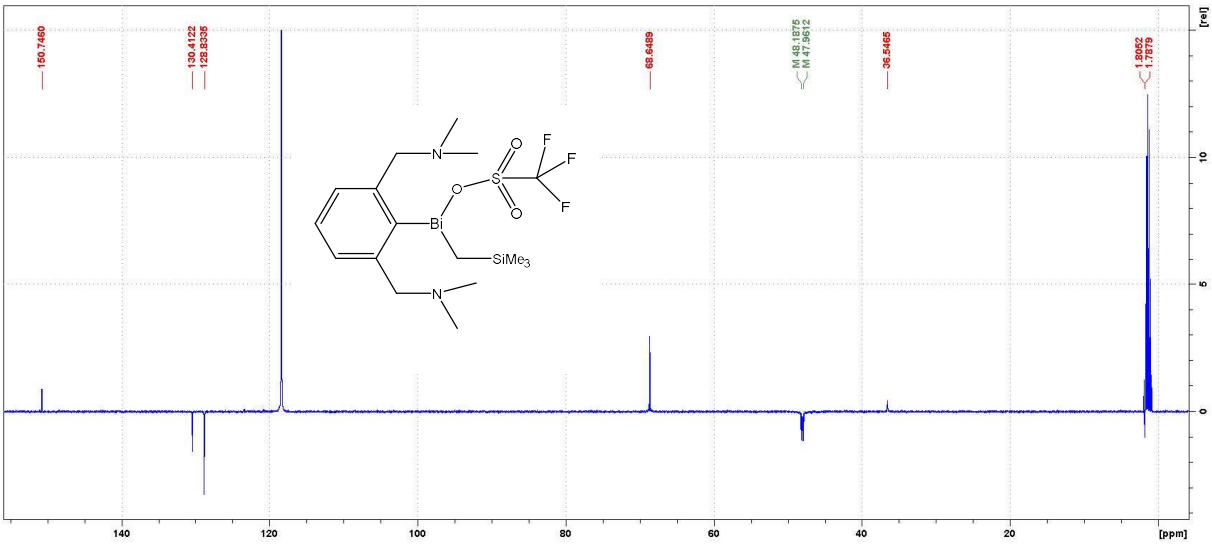

Figure S40. $^{13}C\{^{1}H\}$-APT NMR spectrum of **2g** (125.76 MHz, CD_3CN, 298 K).

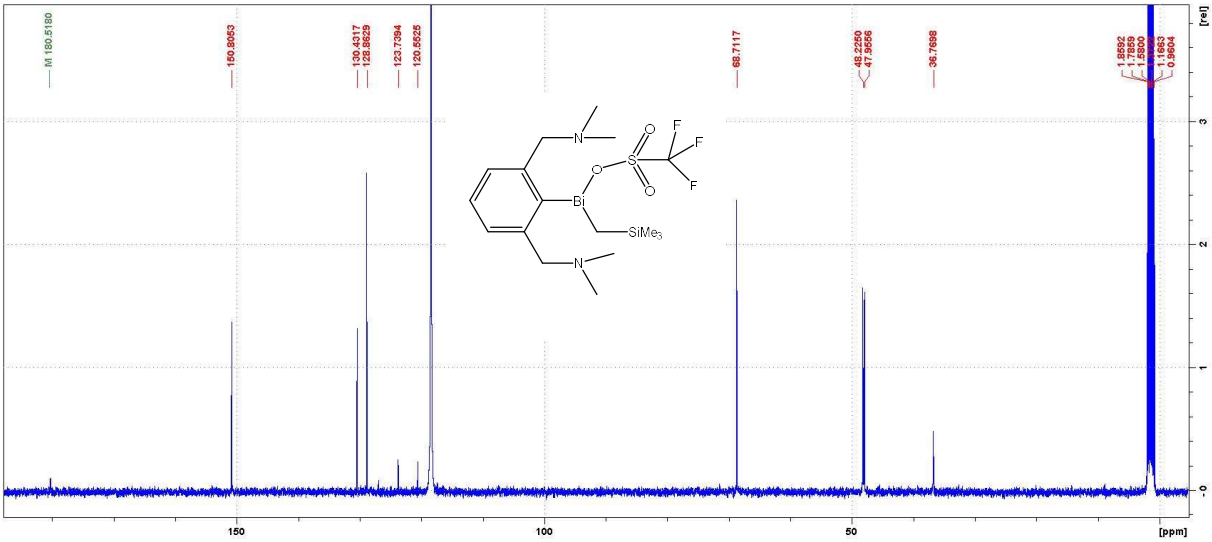

Figure S41. $^{13}C\{^{1}H\}$ NMR spectrum of **2g** (100.61 MHz, CD_3CN, 298 K).

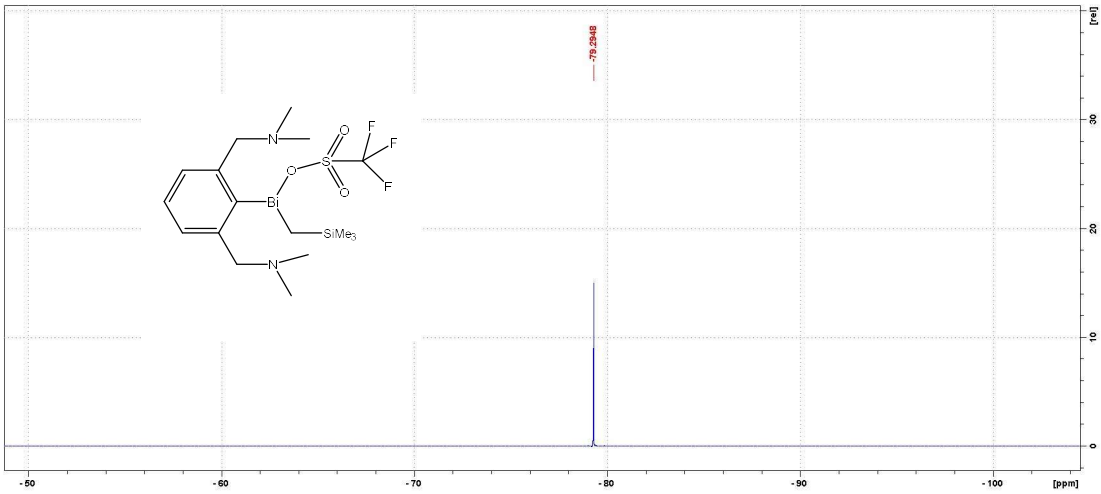

Figure S42. $^{19}F\{^{1}H\}$ NMR spectrum of **2g** (376.5 MHz, CD_3CN, 298 K).

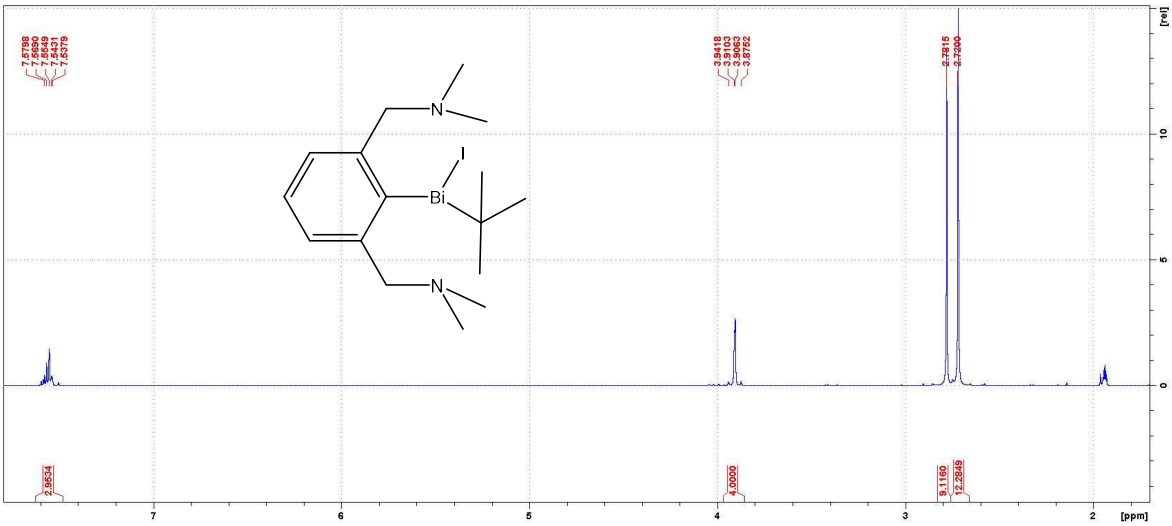

Figure S43. ^{1}H NMR spectrum of **2h** (500 MHz, CD_3CN, 298 K).

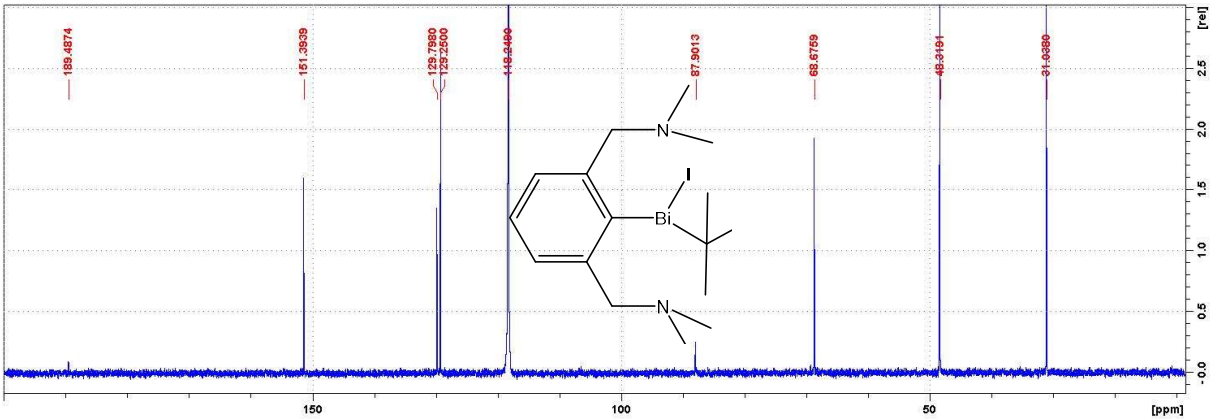

Figure S44. $^{13}C\{^{1}H\}$ NMR spectrum of **2h** (100.61 MHz, CD_3CN, 298 K).

NMR spectra of relevant reaction mixtures mentioned in the discussion and description of other experiment performed.

Synthesis of [2,6-(tBuNCH)$_2$C$_6$H$_3$]BiI$_2$

To a solution of [2,6-(*t*BuNCH)$_2$C$_6$H$_3$]Bi 255 mg (0.56 mmol) in thf (10 mL) a solution of I_2 142 mg (0.56 mmol) was added at r.t. The reaction turned to yellow colour and was stirred for additional 30 min. The solution was evaporated and the residue was washed with hexane (5 mL). The yellow precipitate was crystallized from hot acetonitrile to give [2,6-(*t*BuNCH)$_2$C$_6$H$_3$]BiI$_2$, 304 mg, (77 %), m. p. 285°C(dec.). **^{1}H NMR** (500 MHz, $CDCl_3$) δ (ppm): 1.64 [18H, s, (C*H*$_3$)$_3$C]; 7.91 [1H, t, $^3J(^1H,^1H)$ = 7.6 Hz, Ar-*H*4]; 8.15 [2H, d, $^3J(^1H,^1H)$ = 7.6 Hz, Ar-*H*3,5]; 9.44 [2H, s, C*H*=N]. **^{13}C{^{1}H} NMR** (125.76 MHz, CD_3CN) δ (ppm): 32.0 [(*C*H$_3$)$_3$C]; 62.2 [(CH$_3$)$_3$*C*]; 129.6 [Ar-*C*4]; 136.7 [Ar-*C*3,5]; 149.1 [Ar-*C*2,6]; 168.7 [*C*H=N]; [Ar-*C*1] not detected. **Positive-ion ESI-MS**: m/z 579.0692 $[C_{16}H_{23}N_2BiI]^+$ (100%), mass error -2.1 ppm. **Negative-ion ESI-MS**: m/z 126.9045 $[I]^-$ (100%), mass error -3.9 ppm.

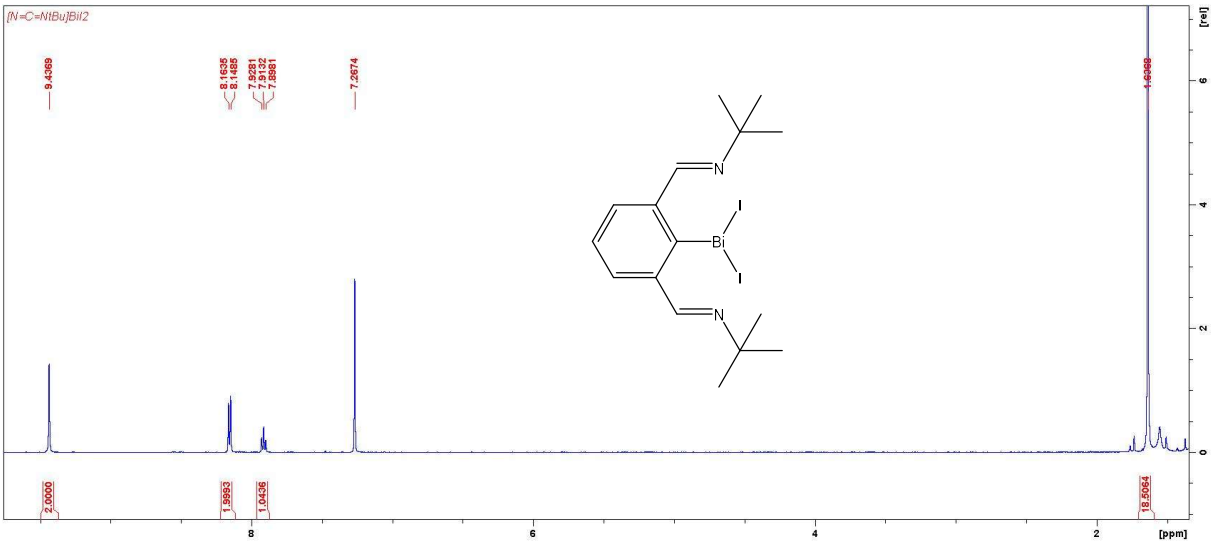

Figure S45. ^{1}H NMR spectrum of [2,6-(tBuNCH)$_2$C$_6$H$_3$]BiI$_2$ (500 MHz, $CDCl_3$, 298 K).

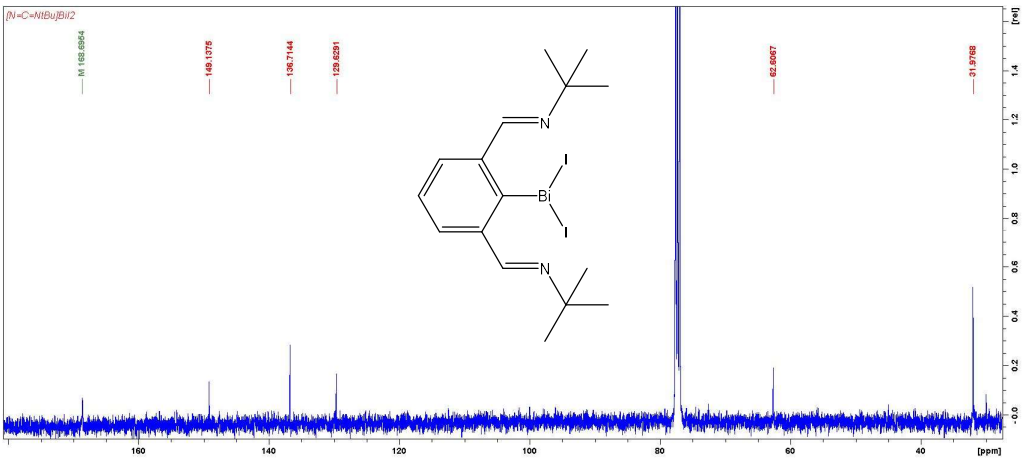

Figure S46. $^{13}C\{^{1}H\}$ NMR spectrum of $[2,6\text{-}(tBuNCH)_2C_6H_3]BiI_2$ (100.61 MHz, $CDCl_3$, 298 K).

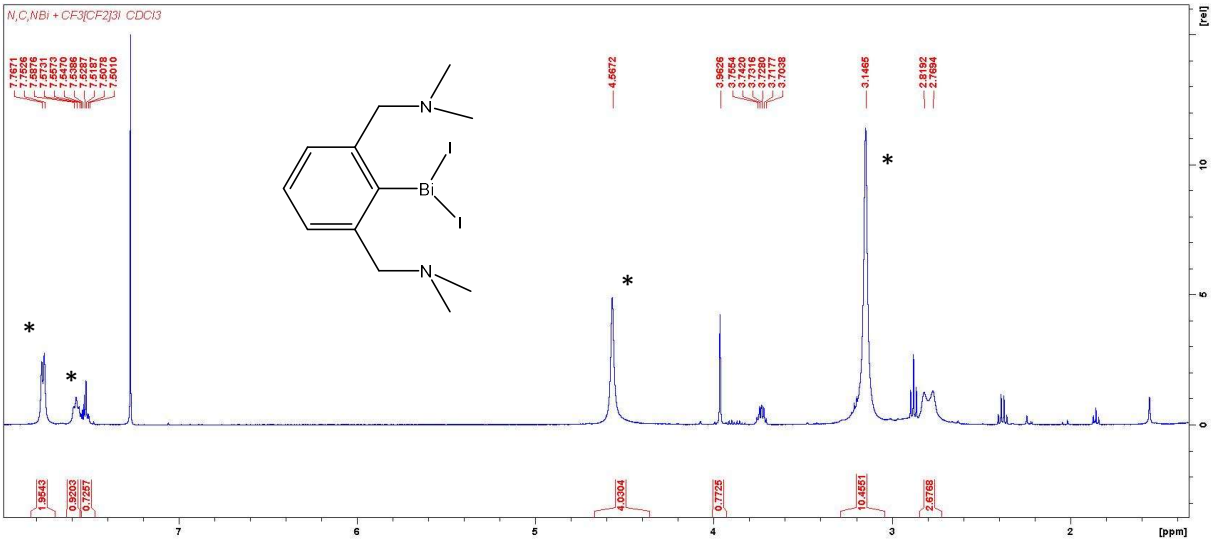

Figure S47. ^{1}H NMR spectrum of mixture of products after reaction of **2** and $CF_3(CF_2)_3I$ (500 MHz, $CDCl_3$, 298 K). The signals of $[2,6\text{-}(Me_2NCH_2)_2C_6H_3]BiI_2$ are marked with *.

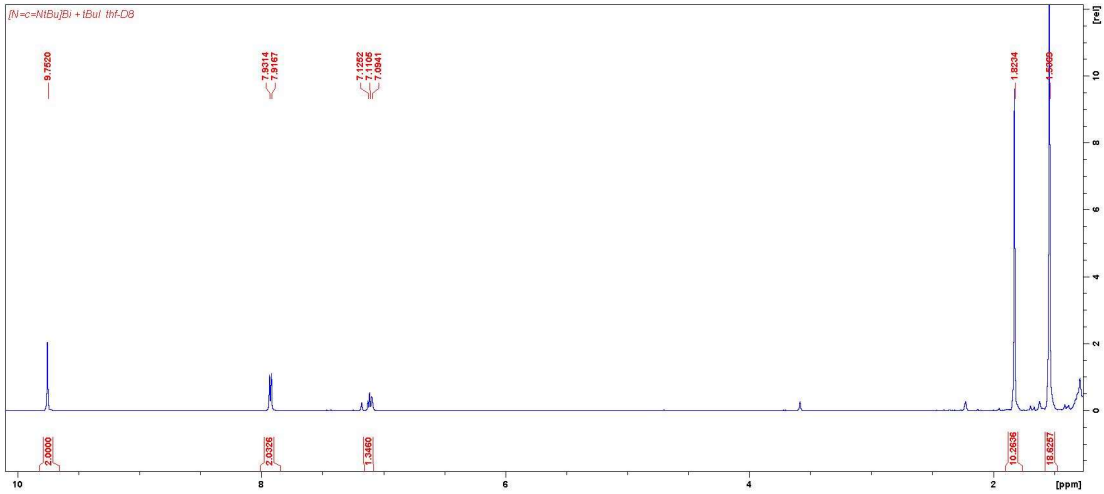

Figure S48. ^{1}H NMR spectrum of mixture of **1** and *t*BuI after five minutes (500 MHz, thf-d8, 298 K).

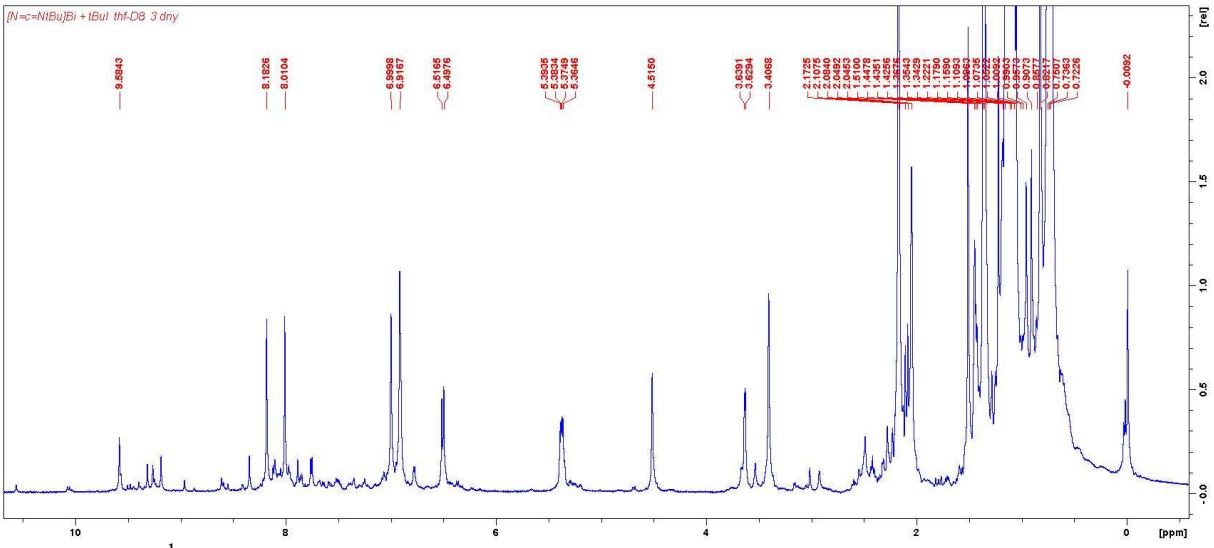

Figure S49. ^{1}H NMR spectrum of mixture of **1** and *t*BuI after three days showing complex mixture (500 MHz, thf-d8, 298 K).

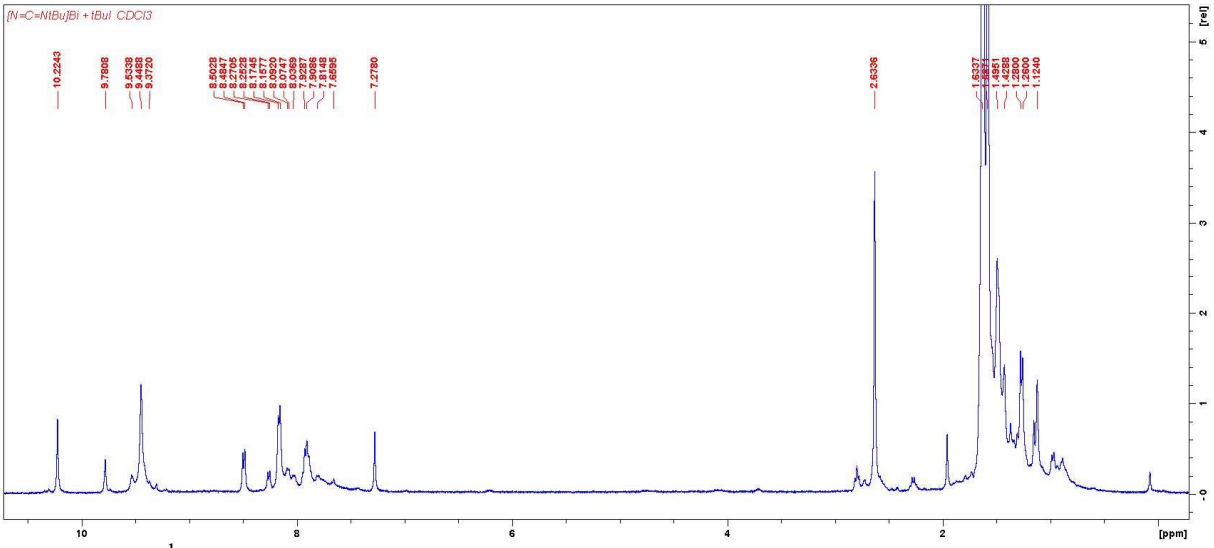

Figure S50. ^{1}H NMR spectrum of insoluble material in thf after reaction of **1** and *t*BuI after three days (400 MHz, $CDCl_3$, 298 K).

Crystals and refinement details of studied compounds.

Table S1. Crystal data and structure refinement of **1c – 1g.thf**.

	1c	**1d**	**1g.thf**
Formula	$C_{18}H_{25}BiF_3IN_2$	$C_{19}H_{27}BiF_3IN_2$	$C_{25}H_{42}BiF_3N_2O_4SSi$
Formula weight, g mol^{-1}	662.28	676.30	760.73
Crystal system	Monoclinic	Monoclinic	Orthorhombic
Crystal size, mm	0.27 × 0.15 × 0.11	0.22 × 0.17 × 0.17	0.44 × 0.29 × 0.13
Space group	$P2_1/c$	$P2_1/n$	$Pca2_1$
a, Å	8.5041(6)	10.1675(4)	18.2488(10)
b, Å	24.5334(17)	16.7465(5)	10.8220(5)
c, Å	10.3325(7)	13.4279(5)	15.7321(9)
α, º	90	90	90
β, º	95.472(2)	97.668(2)	90
γ, º	90	90	90
V, Å^3	2145.9(3)	2265.92(14)	3106.9(3)
Z	4	4	4
ρ_{calcd}, Mg m^{-3}	2.050	1.982	1.626
μ (Mo $K\alpha$), mm^{-1}	9.683	9.172	5.830
F(000)	1240	976	1512
θ range, deg	1 to 27.5	1 to 27.5	2.24 to 30.07
Index ranges	$-11 \le h \le 12$	$-13 \le h \le 13$	$-23 \le h \le 23$
	$-35 \le k \le 36$	$-21 \le k \le 21$	$-14 \le k \le 12$
	$-14 \le l \le 14$	$-17 \le l \le 17$	$-19 \le l \le 20$
No. of reflns collected	55430	38886	26740
No. indep. Reflns	6635	5239	7303
No. obsd reflns with ($I>2\sigma(I)$)	4519	4509	5571
No. refined params	242	241	344
GooF (F^2)	1.139	1.243	1.050
R_1 (F) ($I > 2\sigma(I)$)	0.0618	0.0457	0.0439
wR_2 (F^2) (all data)	0.0804	0.0860	0.0880
Largest diff peak/hole, e Å^{-3}	1.432 / –3.594	1.531 / –2.842	9.639 / –9.111
CCDC	1990145	1990144	1990140

$R_{int} = \sum |F_o^2 - F_{o,mean}^2| / \sum F_o^2$, $S = [\sum(w(F_o^2 - F_c^2)^2)/(N_{diffrs} - N_{params})]^{½}$ for all data, $R(F) = \sum ||F_o| - |F_c|| / \sum |F_o|$ for observed data, $wR(F^2) = [\sum(w(F_o^2 - F_c^2)^2)/(\sum w(F_o^2)^2)]^{½}$ for all data.

Table S1 (continue). Crystal data and structure refinement of **2a – 2c**.

	2a	**2b**	**2c**
Formula	$C_{13}H_{22}BiIN_2$	$C_{14}H_{22}BiF_3N_2O_3S$	$2(C_{14}H_{21}BiF_3N_2)I_2$ $1.5(C_2H_3N)$
Formula weight, g mol^{-1}	542.20	564.37	1281.99
Crystal system	Orthorhombic	Monoclinic	Triclinic
Crystal size, mm	0.53 × 0.53 × 0.25	0.27 × 0.26 × 0.17	0.59 × 0.35 × 0.11
Space group	Pbca	C2/c	P-1
a, Å	11.9179(3)	20.4831(4)	10.5569(8)
b, Å	13.2973(5)	9.6035(3)	11.9145(8)
c, Å	20.3677(7)	19.3496(7)	16.7549(12)
α, º	90	90	75.682(3)
β, º	90	103.9250(10)	87.046(4)
γ, º	90	90	86.095(4)
V, Å^3	3227.79(18)	3694.4(2)	2035.9(3)
Z	8	8	2
ρ_{calcd}, Mg m^{-3}	2.232	2.029	2.091
μ (Mo $K\alpha$), mm^{-1}	12.822	9.701	10.203
F(000)	2000	2160	1194
θ range, deg	1 to 27.5	1 to 27.5	2.24 to 30.07
Index ranges	$-16 \le h \le 16$	$-26 \le h \le 26$	$-13 \le h \le 13$
	$-18 \le k \le 18$	$-12 \le k \le 12$	$-15 \le k \le 15$
	$-27 \le l \le 29$	$-25 \le l \le 25$	$-21 \le l \le 21$
No. of reflns collected	32045	47265	61645
No. indep. Reflns	5029	4254	9461
No. obsd reflns with ($I>2\sigma(I)$)	3423	3726	6422
No. refined params	112	222	415
GooF (F^2)	1.051	1.118	1.043
R_1 (F) ($I > 2\sigma(I)$)	0.0631	0.0286	0.0697
wR_2 (F^2) (all data)	0.1255	0.0590	0.176
Largest diff peak/hole, e Å^{-3}	4.815 / –6.026	1.952 / –1.537	9.035 / –3.568
CCDC	1990147	1990141	1990146

$R_{int} = \sum |F_o^2 - F_{o,mean}^2| / \sum F_o^2$, $S = [\sum(w(F_o^2 - F_c^2)^2)/(N_{diffrs} - N_{params})]^{½}$ for all data, $R(F) = \sum ||F_o| - |F_c|| / \sum |F_o|$ for observed data, $wR(F^2) = [\sum(w(F_o^2 - F_c^2)^2)/(\sum w(F_o^2)^2)]^{½}$ for all data.

Table S1 (continue). Crystal data and structure refinement of **2f** and **2h**.

	2f	**2h**
Formula	$C_{17}H_{30}BiIN_2$	$C_{16}H_{28}BiIN_2$
Formula weight, g mol^{-1}	598.31	584.28
Crystal system	Orthorhombic	Monoclinic
Crystal size, mm	0.44 × 0.32 × 0.24	0.59 × 0.58 × 0.22
Space group	Pccn	$P2_1/c$
a, Å	16.9500(4)	13.4106(6)
b, Å	25.1810(7)	9.8275(5)
c, Å	9.4023(3)	14.9631(8)
α, º	90	90
β, º	90	107.896(2)
γ, º	90	90
V, Å^3	4013.07(19)	1876.61(16)
Z	8	4
ρ_{calcd}, Mg m^{-3}	1.981	2.068
μ (Mo $K\alpha$), mm^{-1}	10.323	11.035
F(000)	2256	1096
θ range, deg	1 to 27.5	1 to 27.5
Index ranges	$-22 \le h \le 21$	$-17 \le h \le 17$
	$-32 \le k \le 32$	$-13 \le k \le 13$
	$-12 \le l \le 12$	$-20 \le l \le 19$
No. of reflns collected	34887	49833
No. indep. Reflns	4613	4662
No. obsd reflns with ($I>2\sigma(I)$)	3966	4117
No. refined params	197	189
GooF (F^2)	1.080	1.116
R_1 (F) ($I > 2\sigma(I)$)	0.0293	0.0536
wR_2 (F^2) (all data)	0.0605	0.1435
Largest diff peak/hole, e Å^{-3}	1.366 / –2.178	7.592 / –5.853
CCDC	1990148	1990142

$R_{int} = \sum |F_o^2 - F_{o,mean}^2| / \sum F_o^2$, $S = [\sum(w(F_o^2 - F_c^2)^2)/(N_{diffrs} - N_{params})]^{½}$ for all data, $R(F) = \sum ||F_o| - |F_c|| / \sum |F_o|$ for observed data, $wR(F^2) = [\sum(w(F_o^2 - F_c^2)^2)/(\sum w(F_o^2)^2)]^{½}$ for all data.

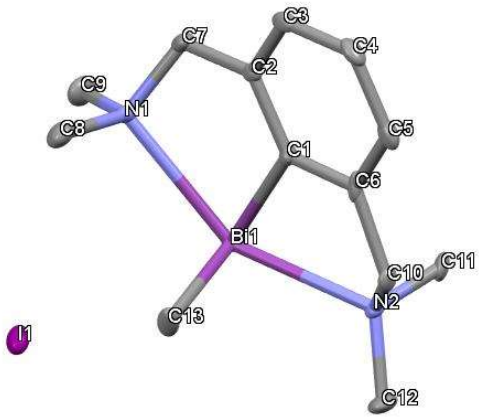

Figure S51. Molecular structure of **2a**.

Table S2. List of elemental compositions, experimental and theoretical m/z values together with calculated mass errors of particular ions observed in positive-ion and negative-ion mass spectra for studied compounds **1a-g** and **2a-h**.

	Positively charged ions (cationic parts)				Negatively charged ions (anionic parts)			
No.	**Elemental composition**	**m/z exper.**	**m/z theor.**	**Mass error [ppm]**	**Elemental composition**	**m/z exper.**	**m/z theor.**	**Mass error [ppm]**
1a	$C_{17}H_{26}N_2Bi^+$	467.1895	467.1894	0.2	I^-	126.9051	126.9050	0.8
1b	$C_{17}H_{26}N_2Bi^+$	467.1896	467.1894	0.4	$CF_3SO_3^-$	148.9526	148.9526	0.0
1c	$C_{18}H_{25}N_2F_3Bi^+$	535.1760	535.1768	-1.5	I^-	126.9048	126.9050	-1.6
1d	$C_{19}H_{27}N_2F_3Bi^+$	549.1930	549.1925	0.9	I^-	126.9052	126.9050	1.6
1e	$C_{22}H_{27}N_2F_9Bi^+$	699.1814	699.1829	-2.1	I^-	126.9051	126.9050	0.8
1f	$C_{21}H_{34}N_2Bi^+$	523.2510	523.2520	-1.9	I^-	126.9054	126.9050	3.1
1g	$C_{20}H_{34}N_2SiBi^+$	539.2294	539.2290	0.7	$CF_3SO_3^-$	148.9524	148.9526	-1.3
2a	$C_{13}H_{22}N_2Bi^+$	415.1584	415.1581	0.7	I^-	126.9052	126.9050	1.6
2b	$C_{13}H_{22}N_2Bi^+$	415.1593	415.1581	2.9	$CF_3SO_3^-$	148.9522	148.9526	-2.7
2c	$C_{14}H_{21}N_2F_3Bi^+$	483.1449	483.1455	-1.2	I^-	126.9048	126.9050	-1.6
2d	$C_{15}H_{23}N_2F_3Bi^+$	497.1610	497.1612	-0.4	I^-	126.9049	126.9050	-0.8
2e	$C_{18}H_{23}N_2F_9Bi^+$	647.1524	647.1516	1.2	I^-	126.9055	126.9050	3.9
2f	$C_{17}H_{30}N_2Bi^+$	471.2219	471.2207	2.5	I^-	126.9047	126.9050	-2.4
2g	$C_{16}H_{30}N_2SiBi^+$	487.1984	487.1977	1.4	$CF_3SO_3^-$	148.9529	148.9526	2.0
2h	$C_{16}H_{28}N_2Bi^+$	457.2041	457.2051	-2.2	I^-	126.9055	126.9050	3.9